Long and short-term magma differentiation at Mt. Etna as revealed by Sr-Nd isotopes and geochemical data

V. Di Renzo [(1)], R.A. Corsaro [(2)], L. Miraglia [(2)], M. Pompilio [(3)], L. Civetta [(4)]

(1) Dipartimento di Ingegneria Civile, Design, Edilizia e Ambiente, Università degli Studi della Campania Luigi Vanvitelli, via Roma 29, 81031 Aversa (CE), Italy

(2) INGV, Sezione di Catania - Osservatorio Etneo, piazza Roma 2, 95125 Catania, Italy

(3) INGV, Sezione di Pisa, via della Faggiola 32, 56126 Pisa (Italy)

(4) Dipartimento di Scienze della Terra, dell'Ambiente e delle Risorse, Università di Napoli Federico II, Largo San Marcellino 10, 80138 Napoli, Italy

Corresponding author:

Rosa Anna Corsaro

INGV- sezione di Catania, Osservatorio Etneo

piazza Roma 2, 95125 Catania, Italy

e-mail: rosanna.corsaro@ingv.it

phone: +39957165800

orcid.org/0000-0001-6137-8806

Abstract

Mt. Etna, in Sicily (Italy), produces effusive and explosive eruptions from summit craters and flanks. Petrology of erupted products has proved fundamental to explore the relationship between magma dynamics within the plumbing system and eruptive styles. Data of Sr-Nd isotopes are quite scarce if compared with the great number of chemical analyses carried out in products of last decades. We measure Sr-Nd isotopes, major and trace elements in products emitted from 2001 to 2012, and consider also published analyses of the 1995 to 2001 eruptions, because carried out in the same laboratories of 2001-2012 ones. Furthermore, we take into account other published analyses extending back to the 14th century, even if performed by different facilities. Based on this dataset, magma dynamics operating at different timescales inside the volcano's plumbing system have been explored. Our analyses evidence that, from 2001 to 2012, three magma types are present in the volcano's plumbing system: i) a deep and poorly evolved basaltic and K-trachybasaltic magma, enriched in radiogenic Sr and LILE, erupted during the 2001 and 2002-03 flank activity; ii) a shallower more evolved K-trachybasaltic magma, less enriched in radiogenic Sr, feeding both summit and flank eruptions and iii) an uncommon, and scarcely radiogenic hawaiitic magma, LILE poor, emitted exclusively from a small sector of the 2002-03 eruptive fissures. By considering a broader time scale, from 14th to 21st century, we conclude that: i) different magmatic components are present in the deep volcano's plumbing system, at about 10-12 km b.s.l; ii) a decoupling of geochemical and isotopic features in magmas stored at different depths is observed after the 1974 flank eruption up to date; iii) mixing between different magmas is an efficient magmatic process to produce magma differentiation at Mt. Etna, regardless of the investigated temporal scale.

***Keywords**: Mt. Etna, Sr-Nd isotopes, bulk rocks composition, volcano plumbing system, magma differentiation, magma mixing*

1. Introduction

Mt. Etna is a basaltic strato-volcano located on the eastern coast of Sicily (Italy), at the outermost margin of the Apennine–Maghrebian belt originated by the convergence of African-Adriatic and Ionian crust with the European one (Bousquet and Lanzafame 2004). Mt. Etna produces both summit and flank eruptions that are principally controlled by magma rise in central conduits (e.g., Rittmann 1965; Wadge,1980; Ryan,1988; Chester et al. 1985; Allard et al. 2006; Corsaro et al.,2009b). Since historic times, "summit eruptions" occur at the open exit of the central conduits, i.e. at the summit craters (Fig.1), that are named: the Southeast Crater and its new cone informally called New Southeast Crater (resulting cone SEC-NSEC), the Northeast Crater (NEC), the Voragine Crater (VOR) and the Bocca Nuova Crater (BN). Summit eruptions may also take place at the subterminal branching of the central conduits. The summit eruptions produce Strombolian explosions and lava fountains, often accompanied by lava flows emission. "Flank eruptions", less frequent than summit ones (Branca and Del Carlo 2004), are mostly driven by fracturing of the central conduits and radial magma drainage. The eruptive fissures opened on the flanks of the volcano generate lava flows of sometimes considerable volume (Branca and Abate 2017). A limited number of flank eruptions (e.g 1763, 1974, 2001, 2002-03) are characterised by a higher explosivity, i.e. large ratio between volume of explosive and effusive products (Rittmann 1965, Tanguy 1980). These types of eruptions were initially classified as ''eccentric'' (Rittmann 1965, Tanguy 1980, Armienti et al. 1988) or ''peripheral'' (Acocella and Neri 2003), but were later renamed as ''deep dike-fed'' (DDF) eruptions (Corsaro et al. 2009b) to highlight their peculiarity since they are supplied by dikes that bypass the shallow plumbing system of the volcano (Rittmann 1965; Armienti et al. 1988; Acocella and Neri 2003; Spilliaert et al. 2006; Corsaro et al. 2009b and references therein).

Petrology of erupted product has resulted to be a key element to recognize depth of provenance and to track the ascent path of magma within the plumbing system (Tanguy 1980, Armienti et al.1988, Andronico et al. 2005, Corsaro et al. 2007). Literature data have shown that volcanics erupted from

summit and during most of flank eruptions consist of highly porphyritic (P.I. >20% vol) and plagioclase-rich, partially degassed K-trachybasalts or hawaiites (Armienti et al. 1989, 2013; Corsaro and Pompilio 2004; Métrich et al. 2004; Spilliaert et al. 2006; Corsaro et al. 2007, 2009a, 2013; Viccaro et al. 2006, 2010, 2016; Ferlito et al. 2012; Giacomoni et al. 2012, 2014, 2016; Kahl et al., 2013, 2015; Corsaro and Miraglia 2014; Mollo et al. 2015, 2018; Perinelli et al. 2016; Corsaro et al. 2017). Magma acquires these petrochemical features after a storage in a shallow region of the volcano's plumbing system (<5 km b.s.l. Mètrich and Rutherford 1998; Mètrich et al. 2004) and is erupted through the central conduits system and strictly related fissures (hereafter it is indicated as CC-type, following Corsaro et al., 2009b). On the contrary highly explosive flank eruptions are fed by a nearly aphyric (P.I. <20% vol) and plagioclase-poor, volatile-rich basaltic and K-trachybasaltic magma (DDF-type); (Andronico et al. 2005; Viccaro et al. 2006; Corsaro et al. 2007; Ferlito et al. 2009a, 2009b, 2012; Ferlito and Lanzafame 2010; Giacomoni et al 2014; Fornaciai et al. 2015, Ubide and Kamper 2018) that ascends from a deeper region (about 10-12 km b.s.l.) of the plumbing system (Spilliaert et al. 2006; Corsaro et al. 2009b). During the 2001 and 2002-03 flank eruptions singular conditions occurred, since both CC-type and DDF-type magmas were contemporaneously erupted. According to Andronico et al. (2005) and Corsaro et al. (2007), DDF-type magma was emitted from Lower Vents (LV) in 2001 and Southern Fissures (SF) in 2002-03, whereas CC-type magma fed the activity of Upper Vents (UV) in 2001 and Northern Fissures (NF) in 2002-03.

The knowledge on such a complex plumbing system, already postulated by Alfred Rittman in 1965, has improved since a regular monitoring of the volcano has been established (Bonaccorso et al., 2004, and referenced therein) and data from petrologic monitoring have been integrated with geophysical measurements, in order to investigate the relationship among pre-eruptive magma dynamics, volcanic activity and tectonics (Corsaro et al., 2013; Palano et al., 2017).

In spite of the huge amount of chemical analyses produced for the recent eruptions of the last decades, measurements of Sr-Nd isotopes, are quite scarce. Furthermore, published analyses are often difficult to be integrated due to the analytical bias of different laboratories. To overcome these limitations, we

measured Sr-Nd isotopes, major and trace elements of the products erupted from 2001 to 2012. The new data have been integrated with published analyses (period 1995-2001) carried out in the same laboratories which analyzed the 2001-2012 ones (Corsaro et al., 2013) Finally, we considered literature data extending back to the 14th century. The overall dataset has been the pillar on which we built a discussion about i) distinct "magma types" residing in the different portion of the volcano's plumbing system and changing over time, ii) compositional variability of magma on a short time (years/months) and long (decades/centuries) timeframe and finally, iii) magmatic processes responsible of magma differentiation at Mt. Etna.

1.1 Eruptive activity

The volcanic activity of Mt. Etna from 2001 to 2012 consisted of both flank eruptions (2001, 2002-03, 2004-05 and 2008-09) and summit activity from three of the four summit craters, namely BN, NEC and the SEC-NSEC, this last being the most active. Brief descriptions of the eruptions are given here, since more complete information is available in the large number of papers dedicated. After a period of summit activity from 1995 to July 2001, (Calvari et al. 1994, 2003; Coltelli et al. 1998, 2000; Corsaro and Pompilio 2004), the volcano resumed its flank activity on 18 July 2001 (Corsaro et al. 2007 and references therein), through a complex system of eruptive fissures cutting the NE and S flanks (Fig. 1). Lava flows and explosive activity (lava fountains, Strombolian and minor phreatomagmatic explosions) clustered in the southern sector of eruptive fissures, at about 2550 and 2100 m a.s.l (Lower vents, LV, Corsaro et al. 2007). Almost simultaneously, the upper portion (above 2600 m a.s.l) of the southern and the north-eastern sectors of eruptive fissures (indicated on the whole as Upper vents, UV Corsaro et al. 2007) were active, producing mainly lava flows effusion.

Summit activity resumed in June-July 2002 with mild Strombolian explosions at NEC and BN (Fig. 1), lasting for about three months (Allard et al. 2006).

Flank activity began again on 26 October 2002, with strong Strombolian explosions and discontinuous lava flow output from eruptive fissures opened nearly simultaneously on the NE and S

flanks (Fig.1) of the volcano (respectively Northern and Southern fissures, namely NF and SF of Andronico et al. 2005), until 5 November 2002. After this date, the emission localized exclusively on the S flank, with continuous explosive activity and lava effusion until 28 January 2003.

After 20 months of quiescence, a new flank eruption started on 7 September 2004, when a complex fracture zone extended (Fig. 1) from SEC towards the Valle del Bove. Several eruptive vents progressively opened downward at 2920, 2820, 2620 and 2320 m a.s.l. and fed a compound lava field until 8 March 2005, when the eruption ended (Burton et al. 2005; Neri and Acocella 2006; Corsaro et al. 2009a).

A two-stage summit activity resumed at SEC during 2006 (Behncke et al. 2008). Indeed, from 14 to 24 July, Strombolian explosions and effusive activity took place from a fissure cutting the lower ESE flank of the SEC cone; in a second phase, from 31 August to 14 December (Calvari and Behncke 2006, 2007; Calvari et al. 2006), Strombolian explosions and periodic lava effusions were produced from vents close to the SEC cone.

Seven paroxysmal episodes occurred at SEC from 29 March 2007 to 10 May 2008 (Bonaccorso et al. 2011). Episode were characterized by vigorous lava fountains, lava flows effusion around the SEC, and emission of ash plume spreading across wide areas of the volcano's flanks. Just three days after the last paroxysm, a new flank eruption started on 13 May 2008 from a complex fissure system opened in the Valle del Bove (Fig. 1). At the beginning of the eruption, lava fountains and spatter-fed flows formed from the northern sector of the eruptive fissures. Later, the activity propagated southward down to about 2800 m a.s.l., where minor Strombolian explosions and lava flows effusion lasted until 6 July 2009.

During 2010, the SEC (in April), BN (from August to December) and NEC (in November) summit craters were the sites of intermittent Strombolian activity (Patanè et al. 2013).

Between 12 January 2011 and 24 April 2012, the eruptive activity was mostly concentrated at SEC, where 25 paroxysmal episodes took place (Behncke et al. 2014).. The paroxysms, repeated in time, formed a compound lava flow field that covered the upper western flank of the Valle del Bove and

fall-outs of pyroclastic materials that forced the temporary closure of Catania airports, damaged agriculture and affected the health of inhabitants with respiratory/eye problems and skin irritiation. Because of the paroxysmal activity, significant morpho-structural changes affected the summit area, with the formation of a new pyroclastic cone (the New Southeast Crater, NSEC) on the eastern flank of the SEC which, in April 2012, was about 190 m high above the pre-cone surface (Behncke et al, 2014). In June-July 2011, also discontinuous Strombolian explosions and intra-crater lava flows characterized the eruptive activity of BN.

1.2 Petrological background

Petrologic studies have significantly contributed to define the structure of the current Mt. Etna's plumbing system. A wide spectrum of laboratory analyses, geothermobarometric and thermodynamic modelling allowed to estimate depth and time of magma storage and to identify the main magmatic processes causing magma differentiation (Peccerillo, 2017).

Different literature models converge to identify a deep reservoir at the interface between the Hyblean carbonate platform and the underlying crystalline crust (Corsaro et al 2009b; Giacomoni et al 2014), at about 10-12 km b.s.l. On the base of volatile concentrations in melt inclusions of 1974, 2001 and 2002-03 eruptions, it has been confined at about 10-12 km b.s.l. Here a volatile-rich (H_2O=3.4 wt.%), poorly differentiated basaltic magma feeding DDF eruptions, is stored (Métrich et al. 2004; Spilliaert et al. 2006, Corsaro et al. 2009b). The existence of this deep storage zone has also been confirmed by rock textures observations, geochemical and isotopic composition of magmas, thermodynamic modelling and thermobarometry of clinopyroxene-liquid equilibrium (Clocchiatti et al. 2004; Viccaro et al. 2006; Corsaro et al. 2007; Ferlito et al. 2009a, 2009b, 2012, Fornaciai et al., 2015, Ubide and Kamper, 2018, Mollo et al., 2018). Noteworthy, some authors (Ferlito and Lanzafame, 2010; Ferlito et al., 2014; Giacomoni et al 2014; Ferlito, 2017) suggest that the high content of volatiles in deep-seated Mt. Etna's magma is in excess respect to the volume of erupted magma and is related to deeper H_2O flushing.

A storage region of poorly differentiated basaltic-trachybasaltic magma at intermediate depth (about 6 km b.s.l.) is inferred by the study of melt inclusions in 2001 and 2002-03 samples (Metrich et al., 2004; Spilliaert et al 2006). Comparable depth ranges have been provided by textural studies of plagioclase associated with termodynamic modelling (5-6 km b.s.l, Giacomoni et al 2014) and by the integration of geodetic and petrologic data (~7 km b.s.l., Palano et al. 2017). This intermediate ponding zone is probably located at the interface between the Hyblean carbonates and the upper Flyschoid Units beneath the volcano.

Finally, a shallow region of the plumbing system (< 5 km b.s.l) has also been suggested, where a partially degassed trachybasaltic magma, mostly crystallizing plagioclase, is stored. This complex reservoir has been broadly documented by the petrologic investigations of products erupted during recent summit (1995-2001, 2006, 2007 and 2011-2013) and flank activity (2001, 2002-03, 2004-05, 2008-09). They comprehend volatiles content of melt inclusions in olivine (Metrich et al. 2004, Spilliaert et al. 2006), compositional data and thermodynamic simulations (Andronico et al. 2005, Corsaro et al. 2007, 2009a, 2013; Ferlito et al. 2012; Viccaro et al 2015), textural and micro-analytical data on plagioclase crystals (Giacomoni et al., 2014, 2016), mineral chemistry and P-T-fO_2-H_2O modelling (Mollo et al., 2015, 2018), application of a clinopyroxene-based hygrometer (Armienti et al., 2013; Perinelli et al., 2016), integration of seismic, geodetic, and petrological data (Viccaro et al., 2016).

More recently the idea of dynamic plumbing system has been proposed combining kinetic modelling of chemical zoning patterns in olivine crystals with thermodynamic modelling (MELTS) (Kahl et al. 2011, 2013 2015, 2016; Giuffrida and Viccaro,2017). The Authors recognized that multiple interconnected reservoirs exist in the plumbing system, at depth from ~600 MPa up to ~40 MPa, and that are occasionally and temporary activated before an eruptive event.

A general consensus is that magma mixing and fractional crystallization, frequently superimposed, are the main magmatic processes driving the differentiation of mantle-derived magma which continuously replenishes the Etnean plumbing system. Mixing generally involves an evolved resident

magma which is injected by a more primitive and volatile-rich magma This process may occur at different depths, before an eruption or during an ongoing activity, may involve different proportions of distinct magmas and may repeat in time. (Corsaro et al. 2009a, Corsaro and Miraglia 2014; Viccaro 2010, 2015; Andronico and Corsaro 2011; Kahl et al. 2011, 2013, 2015, 2016; Ferlito et al. 2012; Giacomoni et al. 2014, 2016; Mollo et al. 2015; Viccaro et al. 2015; Palano et al., 2017; Ubide and Kamper 2018). Fractional crystallization occurs throughout the whole Etnean plumbing system and involves separation of olivine, plagioclase and clinopyroxene in different proportions (Armienti et al. 2004 ; Spilliaert et al. 2006, Kahl et al. 2011, 2013, 2015; Giacomoni et al. 2012, 2014; Mollo et al. 2015; Giuffrida and Viccaro 2017, Peccerillo 2017).

Other processes en route to the surface may concur to the evolution of the present-day parent magma, as the assimilation of plagioclase-bearing lithologies (Schiavi et al. 2015) and of crustal rocks (Viccaro and Cristofolini, 2008), volatile fluxing with selective element transfer by gaseous phases (Ferlito and Lanzafame, 2010), CO_2 flushing (Spilliaert et al., 2006, Collins et al., 2009, Aiuppa et al., 2010, Giuffrida et al., 2017, Giuffrida et al., 2018, Moretti et al., 2018) and finally H_2O-fluxing in the shallow plumbing system (Moretti et al., 2018).

2. Materials and Methods

Rock samples were collected during the monitoring activity carried out at Istituto Nazionale di Geofisica e Vulcanologia, sezione di Catania, Osservatorio Etneo (INGV-OE). They are mostly lavas and pyroclasts (bombs and lapilli) erupted from July 2001 to April 2012. A mafic xenolith (sample 311002A1) hosted in 2002 products has been also analysed for providing additional information on the roots of the plumbing system. As a matter of fact, Etnean mafic xenoliths have been recently interpreted (Corsaro et al., 2014) as fragments of the high-velocity body (HVB) inferred beneath the volcano by seismic tomography (Patanè et al. 2006).

In Table 1 are reported 32 new analyses of major, trace elements and Sr-Nd isotopes in bulk rock, with also Sr isotopes of separated glasses for two samples (260701B and CNE110702). In Table 2

are reported 26 new analyses of Sr-Nd isotopes in bulk rock, with also Sr isotopes of separated glasses for three samples (260701C, 41102A, 41102B) and Sr isotopes of amphibole and clinopyroxene for one sample (180701A). They have been performed on samples erupted from 2001 to 2009, whose major and trace elements in bulk rocks have been already published (see Reference in Table 2). Finally, published analyses of samples erupted during the 2002-03, 2004-05 flank eruptions and the 2002 summit activity (Corsaro et al. 2009a, auxiliary material) are also considered in this study. Overall, 74 analyses among new, partially published and published ones are discussed. Noteworthy, analytical bias is negligible since all the analyses have been performed in the same laboratories described below.

Major and trace element contents were respectively measured at Centre de Recherches Pétrographiques et Géochimiques (SARM) in Nancy (France) using Inductively Coupled Plasma Optical Emission Spectroscopy (ICP-OES) and Inductively Coupled Plasma Mass Spectrometry (ICP-MS) (Carignan et al. 2001). Analytical uncertainty (1σ) is: <1% for SiO_2 and Al_2O_3, <2% for Fe_2O_3, MgO, CaO, Na_2O, K_2O, <5% for MnO, and TiO_2 and 5–10% for P_2O_5, and<5% for all trace elements except U (<8%).

$^{87}Sr/^{86}Sr$ and $^{143}Nd/^{144}Nd$ ratios were determined on bulk rock samples, separated glasses and milled aggregates of amphibole and clinopyroxene, and measured by Thermal Ionization Mass Spectrometry (TIMS) at the Isotope Geochemistry laboratory of INGV, sezione di Napoli, Osservatorio Vesuviano, by a TRITON TI multi-collector mass spectrometer. Sr and Nd measurements were normalized for mass fractionation effects to $^{86}Sr/^{88}Sr=0.1194$, and to $^{146}Nd/^{144}Nd=0.7219$, respectively. The mean measured value of $^{87}Sr/^{86}Sr$ for the standard NIST–SRM 987 was 0.710215 (2σ =0.000020, N= 99) and that of $^{143}Nd/^{144}Nd$ for the La Jolla standard was 0.511841 (2σ=0.000015, N= 18). The external reproducibility 2σ is calculated according to Goldstein et al. (2003). All Sr and Nd isotopic data have been normalized to the accepted values of $^{87}Sr/^{86}Sr=0.71025$ for NIST-SRM 987, and of $^{143}Nd/^{144}Nd=0.51185$, for La Jolla, respectively. The Sr and Nd blanks were negligible for the

analysed samples during the period of measurements. Details on the techniques used are in Arienzo et al. (2013).

3. Results

3.1 Geochemistry of bulk rocks

The products erupted during the 2001-2012 activity are mostly porphyritic K-trachybasalts and a few basalts (Le Maitre, 2002) (Fig.2). Just a scoria (sample 2002-A), collected at 2477 m a.s.l. along the 2002-03 NF, is a hawaiite (inset of Fig. 2) and corresponds to the "Low-potassium oligophyric volcanics" (LKO) of Ferlito et al. (2009a). Actually, hawaiitic to trachitic magmas belonging to Na-alkalic series typically fed the activity of Etna until the eruption of 1971, but were no longer erupted (or at least sampled) later. Their occurrence in the studied period, though representing an important element to define the complexity of the volcano's recent plumbing system, is limited to a single lava flow with a very small volume (10^4 m^3) from a single and isolated vent along the fissure.The less evolved magma (SiO_2 recalculated on a water-free basis is 46.75 wt.%; Na_2O+K_2O= 4.65 wt.%), was erupted from the 2002-03 SF, whereas the most differentiated one (SiO_2 = 49.65 and Na_2O+K_2O =6.29 wt.%) was the hawaiitic sample 2002-A.

The degree of magma evolution is represented by Mg# [=Mg/(Mg+Fe^{2+}) moles, assuming Fe^{3+}/Fe^{2+}=0.2, Middlemost 1989] vs. SiO_2, CaO, alkali (Fig. 3a, b, c) and Th vs. Rb, La and Ni (Fig. 3d, e, f). Data evidence (Fig. 3) that the most basic products are basalts and K-trachybasalts erupted during 2001 and 2002-03, respectively from the LV and SF. A notable compositional variability in terms of both major and trace elements characterizes the products of the 2002-03 eruption. Indeed, the products emitted during other flank eruptions, such as 2001, 2004-05 and 2008-09, are overall more homogeneous. Summit activity from 2002 to 2012 produced variously differentiated magmas but not so basic as the 2001 LV and the 2002-03 SF ones. The comparison with the products erupted during the summit activity of the previous decade (from 1995 to the onset of 2001 eruption); (Fig. 3, dotted line), shows that the compositional field of the 2001-2012 studied volcanics is extended toward

more basic compositions, represented essentially by the DDF-type magma emitted during 2001 LV and 2002-03 SF eruptions. The hawaiite (Table 1) has lower K and Rb and higher REE, Ba, Sr and Th than the other products of the 2002-03 eruption. According to Ferlito et al. (2009a), this sample is representative of the low-K magma which usually fed the volcanic activity prior to 1971 eruption. In particular, selected trace elements (Rb and Th) overlap the compositional field of magmas emitted from 1928 to 1969 (Fig. 3d). The mafic xenolith shows a medium-grained texture (maximum length of crystals $\leq$4 mm) and is made of plagioclase (68%vol.), clinopyroxene (16 %vol.), olivine (8%vol.), opaque oxides (6%vol.) and scarce amphibole (2%vol.). Its composition is significantly different from the products erupted by the volcano in the studied period and in the previous decade (Fig. 3a-d); values of Mg#, Rb, Ni and alkali are lower and concentrations of La and CaO are higher than 2002-03 hosting lavas. Furthermore, its composition is distinct from other xenoliths embedded in the 2001 and 2002-03 lavas (respectively samples 2001INCL and 02NE05 in Table 1 of Corsaro et al. 2014).

In all the diagrams of Fig. 3, the compatible elements (CaO, Ni) decrease, while the incompatible ones (SiO_2, alkali, Rb, La) increase with differentiation. The patterns are quite scattered, suggesting that observed trends do not represent a simply liquid line of descent from a single parental magma, but may result by more complex processes.

The temporal variation of selected major (CaO/Al_2O_3) and trace (La) elements (Fig. 4a, b) evidences that the magma composition may change significantly at short time scale corresponding to the duration of a single flank eruption, as it is particularly evident for the 2002-03 one. But, the variability is beyond the analytical uncertainty also during the summit eruptions of SEC-NSEC from 2006 to 2008 and, later, from 2011 to 2012. Conversely, BN and NEC in 2002 produces magma with a very homogeneous composition. By changing the time scale and considering the entire 2001-2012 period, the compositional variability appears noticeably resized. Indeed, the magma emitted during both flank and summit activity, is bracketed in the same compositional range ($0.54<CaO/Al_2O_3<0.68$ and $50<La<62$ ppm, Fig. 4).Some products of the 2002-03 eruption plot outside of this range (Fig. 4),

namely the most primitive basalts erupted from SF (CaO/Al_2O_3=0.71 and 0.74; La=41 and 47 ppm) and the hawaiite (CaO/Al_2O_3=0.50; La=77 ppm), i.e. the most evolved magma erupted in the studied period.

3.2 Sr and Nd isotopes of Etnean magmas

Literature data show that, since the 14th century up to present day, the $^{87}Sr/^{86}Sr$ ratio in bulk rocks ranges from 0.70330 to 0.70400, and $^{143}Nd/^{144}Nd$ from 0.51283 to 0.51289, with the highest Sr and lowest Nd isotopic ratios measured on samples from recent activity (Corsaro and Cristofolini 1993, Armienti et al. 2004; Clocchiatti et al. 2004; Viccaro and Cristofolini 2008; Corsaro et al. 2009a,b; Viccaro et al. 2011; Nicotra and Viccaro, 2012; Corsaro et al. 2013).

For the 2001-2006 period in particular, several studies have been performed to define the magmatic components and the processes occurring in the Mt. Etna plumbing system (e.g. Clocchiatti et al. 2004; Corsaro et al. 2009a), or to investigate magma source characteristics (e.g. Coulson et al. 2011; Viccaro et al. 2011).

As regards 2001 and 2002-03 eruptions, Clocchiatti et al. (2004) present geochemical and isotopic data of products whose $^{87}Sr/^{86}Sr$ ratios vary from 0.70353 to 0.70365, with the basaltic samples characterized by the highest ratio measured during the historic period (0.70363 and 0.70365, respectively). The authors suggest that the studied eruptions were triggered by a new magma intrusion (eccentric) coming from a minimum depth of 30 km (ca. 1 GPa), which was similar to the 1974 aphyric basalt, but more enriched in K, Rb, Cs and Ra with a higher $^{87}Sr/^{86}Sr$ ratio.

The Sr–Nd isotope compositions have been determined for representative rocks from 1763 to 2004-05 eruptions (Viccaro and Cristofolini. 2008). The $^{87}Sr/^{86}Sr$ ratios for selected lavas range between 0.703343 and 0.703624, showing a main trend of increasing values vs. time, particularly after the 1971 eruption. The $^{143}Nd/^{144}Nd$ ratios show a limited variability (0.512852-0.512908) and a slight time-dependence opposite to that of $^{87}Sr/^{86}Sr$ ratios.

An integrated study on 2006 eruption products, based on major and trace elements, together with Sr–Pb isotope ratio, has been performed by Nicotra and Viccaro (2012). Mainly the Sr isotopic ratios of the 2006 eruption analysed lavas range between 0.703570 and 0.703608, with the exception of one sample with $^{87}Sr/^{86}Sr$ =0.704000. which is a value that the authors considered rather anomalous for the recent volcanic products erupted at Mt. Etna, being at the limit of the isotopic compositional field defined for this volcano.

The $^{87}Sr/^{86}Sr$ ratio of the 2001-2012 products analysed in this study varies from 0.703414±6 to 0.703666±8 (Table 1 and Table 2); the Sr isotopic value of the mafic xenolith is significantly outside this range, being 0.703462±8. The hawaiite differs from the other samples of the 2002-03 eruption and is the least radiogenic of the studied period ($^{87}Sr/^{86}Sr$ =0.703414±6). $^{143}Nd/^{144}Nd$ ratio varies from 0.512851 to 0.512876, with the Nd isotopic value of the mafic xenolith of 0.512859±5. Sr isotopic composition of glasses separated from selected samples of 2001 LV and UV, 2002 activity of BN and NEC, as well as 2002-03 SF and NF (2 new measurements reported in Table 1, 3 published measurements reported in Table 2), has been analysed, as well as $^{87}Sr/^{86}Sr$ ratio of amphiboles and pyroxenes separated from 2001 LV products (Table 2).

In the $^{87}Sr/^{86}Sr$ vs. time plot (Fig. 5a), the 2001 LV and 2002-03 SF products are the most enriched in radiogenic Sr, and are isotopically similar to the products emitted in the first phase of the 2004-05 eruption (Corsaro et al. 2009a). The products from 2001 UV, 2002 NEC-BN summit activity, 2002-03 NF and 2006 to 2011 summit and flank activity, have a lower Sr isotopic composition until the first half of 2011, with $^{87}Sr/^{86}Sr$ similar to the magmas of Mt. Etna volcanic activity emitted at the end of the 2004-05 eruption. Noteworthy, the Sr isotopic ratio starts to increase from July 2011, with the maximum value measured for the sample CSE290811C ($^{87}Sr/^{86}Sr$ = 0.703589±6). The $^{87}Sr/^{86}Sr$ ratio of the hawaiite and of the mafic xenolith are beyond the range of the Sr isotopic compositions of all the other samples. Volcanic glasses show an overall equilibrium with the rocks from which they were separated, as is shown by the similarity of their Sr-isotope compositions (Fig. 5a). About mafic minerals, the $^{87}Sr/^{86}Sr$ ratio of clinopyroxene is slightly lower than the host 2001 lavas, but is within

the Sr isotopic range published by Armienti et al. (2007) for the sample July 2001-2550H; amphibole, more radiogenic than clinopyroxene, is in equilibrium with host lava.

The $^{143}Nd/^{144}Nd$ vs. time plot (Fig. 5b) shows a similar but inverse pattern with respect to Sr isotopes. Nd isotopes of 2001 LV, 2002-03 SF rocks and of the first phase of 2004-05 eruption, are characterized by lowest values of $^{143}Nd/^{144}Nd$, whereas the 2001 UV, the 2002 NEC-BN summit activity, the 2002-03 NF, as well as all the summit and flank activity occurring from 2006 to 2012, have significantly higher values. The $^{143}Nd/^{144}Nd$ ratio of the mafic xenolith is within the range of the Nd isotopic compositions of the other samples (Fig. 5b). In conclusion, Sr and Nd isotopic (Fig. 5c) ratios define a negative trend from the $^{87}Sr/^{86}Sr$ enriched magmas erupted from 2001 LV and 2002-03 SF to $^{87}Sr/^{86}Sr$ poorer recent magmas erupted in 2009, 2011 and 2012, and plot in the Etna Sr-Nd field, described by lavas erupted after 1974 (Armienti et al. 2004; Clocchiatti et al. 2004; Viccaro and Cristofolini 2008; Corsaro et al. 2009a; Viccaro et al. 2011; Corsaro et al. 2013).

4. Discussion

We will discuss here the compositional variability of magma on a short time scale (years/months), and then we will contextualise this variability in a longer timeframe (centuries). For both time intervals, we analyse possible relationships between the identified magmatic components and magma dynamics within the plumbing system of the volcano.

4.1 Short-term magma dynamics

4.1.1 Magma types in the Etnean plumbing system (1974 to 2012)

To identify the isotopic components characterising the recent Mt. Etna's plumbing system, we performed a statistical analysis by Isoplot 3.00 software (K.R. Ludwig, bgc.org/isoplot_etc /software .html), made on a large database that combines our Sr isotopic data of the 2001-2012 magmas and published $^{87}Sr/^{86}Sr$ values of Etnean products erupted after 1974 (Armienti et al. 2004, 2007; Clocchiatti et al. 2004; Viccaro and Cristofolini 2008; Corsaro et al. 2009a; Viccaro et al. 2011;

Corsaro et al. 2013). This approach allows distinguishing two distinct modes in the Sr histogram (green solid lines in Fig. 6).

The mode relative to the 67% of Sr isotopic data is centered on a value of $^{87}Sr/^{86}Sr$= 0.703571. The mode relative to the 33% of Sr isotopic data peaks around $^{87}Sr/^{86}Sr$= 0.703635, the most enriched in radiogenic Sr. It is worth noting that a third type (not shown in Fig. 6) is detected by our study, i.e. the least enriched in radiogenic Sr ($^{87}Sr/^{86}Sr$= 0.703414). It is represented exclusively by the 2002-03 hawaiitic magma and, accordingly, it looks like an accessory component of the volcano's plumbing system post 1970s. On the contrary, it was dominant in Etnean magmas erupted before 1970s. Indeed, literature data indicate that historical products erupted from 1329 to 1951 range between 0.70330 and 0.70352 (Corsaro and Cristofolini 1993; Corsaro et al. 1996; Tonarini et al. 1995; Viccaro and Cristofolini, 2008).

The largest group (67%) comprises most of the 2001 to 2012 summit and flank eruptions which are fed by CC-type magma. The secondary mode (33%) is essentially represented by the most basic and radiogenic basaltic DDF-type magma emitted from 2001 LV and 2002-03 SF.

The above isotopic groups are also characterised by distinctive trace element signatures as evidenced by the diagrams isotopes vs. incompatible ratio elements (Fig. 7). The less enriched Sr group, similar to that erupted before 1971 at Mt. Etna, is represented by the 2002-03 hawaiitic sample (2002-A , Table 1) and is characterised (Fig.7a) by the lowest Rb/Nb ratio (0.66), whereas the CC-type shows an intermediate Rb/Nb ratio (average=1.1±0.04) and the DDF-type has the highest Rb/Nb ratio (average=1.2±0.06). Also Rb/Th ratio (Fig.7b) is high (average=6.6±0.5) for the DDF-type, intermediate for the CC one (6.1±0.4) and low (3.7) for the hawaiitic 2002-A sample. These values match the results of Corsaro et al. (2009b), who measured for Rb/Th the values: 6.9, 6.1 and 3.8, respectively for DDF, CC and pre-1971 magma. The compositional differences of Sr-isotopes and trace element ratios (Fig. 7), existing among the three above described magma types, result too large to be explained with a simple fractional crystallization process. In particular, DDF and CC-type

magmas are not related by a parental relationship, as previously stated analysing mainly ratios between incompatible elements of a more restricted dataset (Corsaro et al. 2007).

4.1.2 Short-term magmatic processes in the Etnean plumbing system

Petrologic studies conducted over the recent decades have shown that significant geochemical and isotopic variations are evident in products emitted in a short time scale (days-months), generally corresponding to an eruption. These changes can occur within the shallower part of the plumbing system and/or involve also the deeper one, as during the 2001 and 2002-03 eruptions. Diagrams of Figs. 4 and 5 highlight that short-term compositional variability is a feature of 2001-2012 products too. We focus here on two contrasting examples concerning magma erupted by: 1) distinct portions of the eruptive fissures opened during the 2001 and 2002-03 flank eruptions and 2) NEC and BN, which reactivated in June-July 2002, after the 2001 flank eruption.

For the first case, the DDF-type magma erupted from the 2001 LV and 2002-03 SF, remains chemically distinct (Fig.4) from the CC-type erupted from the 2001 UV and 2002-03 NF. Also Sr isotope data of bulk rocks and separated glasses (Fig. 5a) confirm that DDF and CC-types magma emitted during 2001 and 2002-03 flank activity, show different compositional ranges. Then we suggest an independent pathway of magma ascent from distinct reservoirs (Fornaciai et al. 2015), even if magma mixing immediately before and/or during magma uprise has been hypothesized by other authors (Viccaro et al. 2006, Ferlito et al.,2009a, b).

For the second case, the Sr isotopic values measured in products of NEC from June to July 2002, vary from 0.703593 to 0.703636 (Fig. 8) and are significantly higher than those erupted by this crater in the previous years (1995-1999, Corsaro et al. 2013), ranging from 0.703556 to 0.703569 (Fig. 8). Furthermore, the Sr isotopic composition on separated glass is slightly less radiogenic than the bulk rock (Table 1). We then hypothesize that the NEC compositional variability can be explained with a mixing (Fig. 8) between the most evolved CC-type magma supplying the NEC since 1995 (end member CNE060696, $^{87}Sr/^{86}Sr$=0.703556±6, Nb= 49.1 ppm, complete analysis in Corsaro et al.

2013) and the DDF-type magma feeding the 2001 LV activity (end member 180701A, $^{87}Sr/^{86}Sr$=0.703664±7, Nb= 37.2 ppm, complete analysis in Corsaro et al. 2007). The mixing curve modeled (Faure 1986, p. 142 , equation 9.9) matches well the measured geochemical and isotopical data (Fig. 8). We argue that, in the months following the 2001 flank eruption, the DDF-type magma began to intrude the shallow plumbing system and progressively mixed with the resident CC one. Therefore, we estimate that the CC-type magma erupted during the subsequent activity of NEC in June-July 2002, was mixed with about 40-55% of the 2001 DDF-type (Fig.8) and hence resulted different from the CC-type magma of the previous decade (Fig. 8). Our data confirm the findings of Corsaro et al. (2009b) about the 1974 eruption. In that time, a DDF-type magma was emitted during a flank eruption lasted from January to March 1974; when in October the activity restarted at NEC, the composition of the erupted CC-type magma displayed a 25% imprint of the DDF-type magma, suggesting that DDF-type magma intruded also the shallow part of the plumbing system.

The studies carried out on the products of 2004-05 flank eruption too, confirm the occurrence of pre-eruptive mixing between a CC-type magma and a DDF-type inherited from 2002-03 activity. (Corsaro et al. 2009a, Ferlito et al. 2012; Giacomoni et al. 2014; Palano et al., 2017).

To explain the compositional variability of the products erupted during the activity of SEC from July to December 2006, various authors (Ferlito et al. 2010; Nicotra and Viccaro 2012; Kahl et al., 2013; Giacomoni et al. 2014) agree upon a repeated mixing process between a magma stored in the shallow plumbing system and CO_2-rich magma batches from depth. Similarly, progressive mixing between a fairly evolved magma stored at shallow depth and a more basic deep magma has been hypothesized during the paroxysmal activity of SEC in 2007-08 and the 2008-09 flank eruption (Corsaro and Miraglia 2014). In this study, geochemical and Sr-isotope data clearly show that the products erupted from 2006 to 2009 have typical compositions of CC-type magma (Figs. 3, 4, 5, 7). This evidence suggests that the deep, CO_2-rich and basic magma supposed to supply the shallow plumbing has not the geochemical/isotopic signature of a DDF-type magma Indeed, to our knowledge, the most basic DDF-type magma remains that emitted from SF during the 2002-03 eruption.

Finally, referring to the most recent paroxysmal activity of NSEC from 2011 to 2012, data show that major and trace elements vary significantly (Figs. 3, 4) and Sr isotopes, starting from July 2011, are slightly more radiogenic (Fig. 5a). The compositional variability of 2011-12 NSEC products has been interpreted with the superimposition of gas migration from deep portions of the Etna transport system (Giuffrida et al. 2018), fractional crystallization and mixing in variable proportions of magma stored at shallow depth with more basic magma ascending from intermediate to shallow levels of the plumbing system (Viccaro et al. 2015). Our data indicate that, such as for the 2006-09 period, the more basic magma that repeatedly supplies the shallow plumbing system maintains on the whole the features of a CC-type magma. But, starting from July 2011, a significantly more radiogenic magma starts to be erupted and is therefore present in the shallow region of the volcano's plumbing system. Its occurrence is briefly discussed in the framework of long-term processes described in the next section.

4.2 Long-term magma dynamics

4.2.1 Magmatic components in the Etnean plumbing system (14th-21st century)

We compared (Fig. 9) our data with a larger dataset on the Etnean magmas erupted since 1329 (Corsaro and Cristofolini 1993; Corsaro et al. 1996; Tonarini et al. 2001; Armienti et al. 2004; Viccaro and Cristofolini 2008, Corsaro et al. 2009a, 2013, Nicotra and Viccaro 2012, Correale et al. 2014), which are CC-type magmas of summit and flank activity, as well as the DDF-type of 1763 (La Montagnola), 1974, 2001 (LV) and 2002-03 (SF) eruptions. In diagrams $^{87}Sr/^{86}Sr$ vs. ratios of highly incompatible elements (Fig. 9), DDF-type magmas clearly cluster in two poles, even if some scatter exists because data from different laboratories are considered, and unavoidable analytical bias may occur. A pole is readily identifiable with the DDF-18th century component, since it pertains to the products of the 1763 DDF (La Montagnola) eruption showing the lowest radiogenic Sr isotopic composition ($0.703343 \leq ^{87}Sr/^{86}Sr \leq 0.70342$), and low Rb/Th, Rb/Nb and Rb/La (Fig. 9a, b, c). The opposite pole exhibits higher $^{87}Sr/^{86}Sr$ ($0.703533 \leq ^{87}Sr/^{86}Sr \leq 0.70365$), and higher Rb/Th, Rb/Nb and

Rb/La ratios and is associable with the DDF-21st century component, since it relates to the products of the 2001 and 2002-03 eruptions (Fig. 9a, b, c) . The only DDF-type magma of the 20th century, emitted in 1974, shows compositional features of the DDF-21st century pole. Since we start from the assumption that products of DDF eruptions represent magmas residing in the deep plumbing system, we argue that the DDF-21st component has become present in the root of the Mt. Etna plumbing system at least since 1970s. On the basis of our data, we cannot assert if the DDF-21st century component represents the parental magma which is presently filling the deep plumbing system of the volcano. Really, magmas even with higher Rb/Nb (see Kamentsky et al. 2007) and $^{87}Sr/^{86}Sr$ (Correale et al 2014) than the DDF-21st component have fed the deep part of the plumbing system in the past and were erupted explosively 3930 years ago (Coltelli et al. 2005), thus a possibly more enriched end-member, not yet erupted, cannot be excluded.

4.2.2 Long-term magmatic processes in the Etnean plumbing system

The variation of the Sr isotopic ratio and selected ratios of incompatible elements at the time scales of centuries is shown in Fig. 10. Despite the scatter produced by different analytical laboratories, $^{87}Sr/^{86}Sr$, Rb/Th, and Rb/La show a limited variability until the 20th century, while all these ratios increase significantly (more than 30%) later. This diagram also shows that before the 20th century, DDF and CC-type magmas share the same Sr isotopic compositions and ratios between incompatible elements. If, again, we assume that products of the DDF eruptions are representative of DDF-type magmas residing in the deep plumbing systems, while flank and summit eruptions testify to CC-type magmas tapping the shallow plumbing system, analyses available up to now led to conclude that from the 14th to 20th century the entire Etnean plumbing system was homogeneous and was supplied by a deep magma (DDF-18th century component) with geochemical characteristics that remained uniform over time (Fig.10). The 1974 DDF eruption is the early evidence that the composition of deep magma

is changing (DDF-21st century component), becoming basaltic and K-trachybasaltic, more radiogenic and LILE enriched (Corsaro et al. 2009b).

At that time, however, the compositional features of the shallow and deep parts of the volcano's plumbing system, appears different. Indeed, the CC-type magma feeding the summit activity in 1974 (Fig.10 b, c) continues essentially to keep an "imprint" close the DDF-18th century component, being the contribution of the DDF-21st century component estimated only of 25% (Corsaro et al., 2009b). Magma erupted after 1974 acquires the clear isotopic and geochemical signature of the DDF-21st century component only after 1990; this delay could be explained taking into account that a few decades are necessary so that the new DDF-21st century component intrudes the shallow plumbing system and mix efficiently (Morgavi et al. 2013) with the resident DDF-18th century component. However, the occurrence of magma pockets (e.g. hawaiite erupted from the NE rift in 2002-03 eruption) and/or mafic minerals (e.g. clinopyroxene in 2001 lavas) and/or mafic xenoliths (e.g.sample 311002A1 in 2002-03 lavas) with geochemical signature of DDF 18th century component, suggests that, in the last decades, the volcano's shallow plumbing system is not fully homogeneous. About the studied xenolith, the composition of major and trace elements is rather different from other xenoliths hosted both in 2001 and 2002-03 lavas (Corsaro et al. 2014), which have been interpreted as fragments of the High Velocity Body (HVB, Patanè et al 2006 and references therein) rooted beneath the volcano. Our data evidence that the composition of xenoliths is even more complex than previously assumed (Corsaro et al. 2014), suggesting that cumulitic bodies, compositionally distinct or zoned, occur in the basement of the volcano.

Geochemical decoupling between different portions of the plumbing system and important heterogeneities are rather common in basaltic volcanoes with persistent activity, i.e. Stromboli, (Landi et al., 2009; Pompilio et al. 2012; Francalanci et al., 2012; Bragagni et al., 2014), Kilauea, (Pietruska et al. 1999;Thornber 2003) or Piton de la Fournaise (Di Muro et al., 2014) denoting either i) a complex geometry of the plumbing system, and ii) time scale of geochemical rehomogenization after recharge (or mixing) longer than the residence time. In absence of an imminent DDF eruption

that might provide information on the present-day geochemical signature of the magma at depth, we cannot interpret precisely the return toward less radiogenic compositions shown after the 2004-05 eruption until 2011 (Fig. 5a). This trend might be related to some heterogeneities that are still preserved in the shallow plumbing system, as documented by the eruption of a hawaiitic magma during the 2002-03 flank activity. But, we cannot exclude a return of the DDF-type component that is now feeding the shallow plumbing system toward less radiogenic and less LILE enriched composition. In this complex context, it is intriguing to investigate if the eruption of slightly more radiogenic magmas from 2011 to 2012 (Fig.5a) is casual or instead marks the onset of a further change of magma composition. Indeed, literature data evidence that in the past (15 ka–present) the DDF-type primitive basaltic magmas have modified their composition, probably due to different degrees of melting of a heterogeneous mantle source which experienced several stages of metasomatism (Corsaro and Métrich 2016).

5. Conclusions

We investigated the geochemical and Sr-Nd isotopic compositions of products erupted from 2001 to 2012 at Etna during flank and summit eruptions and integrated them with already published data going back to 14th century. The performed study i) attempts to improve the knowledge of magmatic processes and dynamics that operate at different timescales within Etna's plumbing system and, ii) provides useful information to investigate the behavior of other basaltic volcanoes with persistent activity (e.g., Stromboli, Kilauea, or Piton de La Fournaise), where geochemical decoupling between different portions of the plumbing system are rather common.

Our results highlight that:

– In the period 2001-2012, three magma types are present in the volcano's plumbing system: i) a deep and poorly evolved magma, enriched in radiogenic Sr and LILE (DDF-type), erupted from 2001 LV and 2002-03 SF; ii) a shallower, more evolved magma, less enriched in radiogenic Sr (CC-type), feeding summit craters and flank activity of 2001 UV, 2002-03 NF, 2004-05, 2008-09 and

2002-2012; iii) a scarcely radiogenic magma, not LILE enriched, represented exclusively by a hawaiite emitted from a sector of the 2002-03 eruptive fissures. It is unique in the last 40 years and shares its compositional and isotopic features with the products erupted by the volcano pre-1970s. Its limited volume make this rather more an oddity than a standard component of the Etna magmatic system and represent an isolate magma pocket intruded and rejuvenated by the 2002 N dykes system.

– The analysis, extended to a broader time scale (14^{th}-21^{st} century), allows a more detailed characterization of the volcano's deep plumbing system, whose composition is assumed to be represented by DDF-type magmas. The identified components over time are: i) a DDF-18^{th} century component that pertains to the products of the 1763 (La Montagnola) eruption with the lowest Sr-isotopic composition and lowest LILE; ii) a DDF-21^{st} century component with the highest Sr-isotopic composition and content of LILE, corresponding to the products of 2001 LV and 2002-03 SF eruptions. The DDF-21^{st} century component progressively becomes dominant in the root of the volcano after the 1974 eruption. The magma supply rate at depth and the degree of mixing are probably key factors in controlling the delay necessary for the registration of deep magma compositional changes in the shallow one: in other words the hysteresis of the system. Local tectonic processes that controls magma transport might also influence the rate and efficiency of mixing.

– The 1974 eruption represents a benchmark in the recent history of the volcano. Indeed, a K-trachybasalt, more radiogenic and richer in LILE than the past, was emitted for the first time. Furthermore, after the 1974 eruption, the plumbing system was no longer homogeneous. Geochemical and isotopic decoupling between different portions of the plumbing system began during the 1974 eruption and are still on going to date.

– Mixing between different magmas seems to represent an efficient magmatic process to produce magma differentiation at Mt. Etna, both in the short and long term. It has been documented between variously evolved CC-type magmas stored in the shallow plumbing system, and also between DDF

and CC-type magmas.

– Finally, at least a few points discussed in this paper deserve to be deepened in the future. Indeed a stimulating challenge is to understand the reasons why at Mt.Etna the deep magma is more radiogenic than the shallower one. Noteworthy, this features is inverted at Stromboli where, in the past centuries, the deep magma has always been less radiogenic than the shallow one (Landi et al., 2009, Pompilio et al, 2012). Furthermore, it's also intriguing to explore why the alkali enrichment of Etnean magma occurs just after 1970's. Corsaro and Metrich (2016) noticed that this compositional turning point was accompanied by modifications of volcanological and seismotectonic patterns, but presently all data are faraway to be integrated in a model.

Acknowledgements

We are very grateful to Silvio Mollo and an anonymous reviewer for their helpful comments. A. Gomez-Tuena is acknowledged for editorial handling. Our thanks go to L. Messina for preparing powder for rock analyses. We thank also S. Conway for revising the English language of the manuscript. The geochemical and isotopic analyses were funded by Italian Civil Protection Department (DPC) for the monitoring activity of Sicilian active volcanoes.

References

Acocella, V., Neri, M., 2003. What makes flank eruptions? The 2001 Mount Etna eruption and its possible triggering mechanisms. Bull. Volcanol. 65, 517- 529

Allard, P., Behncke, B., D'Amico, S., Neri, M., Gambino, S., 2006. Mount Etna 1993–2005: anatomy of an evolving eruptive cycle. Earth Sci. Rev. 78, 85-114

Aiuppa, A., Cannata, A., Cannavò, F., Di Grazia, G., Ferrari, F., Giudice, G., Gurrieri, S., Liuzzo, M., Mattia, M., Montalto, P., Patanè, D., Puglisi, G., 2010. Patterns in the recent 2007–2008 activity of Mount Etna volcano investigated by integrated geophysical and geochemical observations. Geochem. Geophys. Geosyst. 1, Q09008

Andronico, D., Branca, S., Calvari, S., Burton, M., Caltabiano, T., Corsaro, R.A., Del Carlo, P., Garfì, G., Lodato, L., Miraglia, L., Murè, F., Neri, M., Pecora, E., Pompilio, M., Salerno, G.,

Spampinato, L., 2005. Multidisciplinary study of the 2002–03 Etna eruption: insights into a complex plumbing system. Bull of Volcanol 67, 314-330

Andronico, D., Corsaro, R.A., 2011. Lava fountains during the episodic eruption of South-East Crater (Mt. Etna) 2000: insights into magma-gas dynamics within the shallow volcano plumbing system. Bull Volcanol 73, 9, 1165-1178

Arienzo, I., Carandente, A., Di Renzo, V., Belviso, P., Civetta, L., D'Antonio, M., Orsi, G., 2013. Sr and Nd isotope analysis at the Radiogenic Isotope Laboratory of the Istituto Nazionale di Geofisica e Vulcanologia, Sezione di Napoli - Osservatorio Vesuviano. Rapporti Tecnici INGV n. 260

Armienti, P., Innocenti, F. , Petrini, R., Pompilio, M., Villari, L., 1988. Sub-aphyric alkali basalt from Mt. Etna: Inferences on the depth and composition of the source magma. Bull Mineral Rend Soc Ital Mineral Petrol 43, 877-891

Armienti, P., Innocenti, F., Petrini, R., Pompilio, M., Villari, L., 1989. Petrology and Sr-Nd isotope geochemistry of recent lavas from Mt. Etna: bearing on the volcano feeding system. J. Volcanol. Geotherm. Res. 39, 315-327

Armienti, P., Perinelli, C., Putirka, K.D., 2013. A New Model to Estimate Deep-level Magma Ascent Rates, with Applications to Mt. Etna (Sicily, Italy). Jour of Petrol 54, 795-813

Armienti, P., Tonarini, S., D'Orazio, M., Innocenti, F., 2004. Genesis and evolution of Mt Etna alkaline lavas: petrological and Sr–Nd–B isotope constraints. Periodico di Mineralogia 73, 29-52

Armienti, P., Tonarini, S., Innocenti, F., D'Orazio, M., 2007. Mount Etna pyroxene as tracer of petrogenetic processes and dynamics of the feeding system. In: Beccaluva, L., Bianchini, G.,Wilson, M.(Eds.), Cenozoic Volcanism in the Mediterranean. Geological Society of America Special Papers 418, pp. 265–276.

Behncke, B., Branca, S., Corsaro, R. A., De Beni, E., Miraglia, L., Proietti, C., 2014. The 2011–2012 summit activity of Mount Etna: Birth, growth and products of the new SE crater. Journal of Volcanology and Geothermal Research 270, 10-21

Behncke, B., Calvari, S., Giammanco, S., Neri, M., Pinkerton, H., 2008. Pyroclastic density currents resulting from interaction of basaltic magma with hydrothermally altered rock: An example from the 2006 summit eruptions of Mount Etna (Italy). Bull Volcanol 70, 1249-1268

Bonaccorso, A., Calvari, S., Coltelli, M., Del Negro, C., Falsaperla, S. (Eds.), 2004. Mt. Etna: Volcano Laboratory. Geophys. Monogr. Ser., vol. 143, 369 pp., AGU, Washington, D. C.

Bonaccorso, A., Bonforte, A., Calvari, S., Del Negro, C., Di Grazia, G., Ganci, G., Neri, M., Vicari, A., Boschi, E., 2011. The initial phases of the 2008–2009 Mount Etna eruption: A multidisciplinary approach for hazard assessment. J. Geophys. Res. 116, B03203

Bousquet, J.C., Lanzafame, G., 2004. The tectonics and geodynamics of Mount Etna: synthesis and interpretation of geological and geophysical data. in Mt. Etna: Volcano Laboratory, Geophys. Monogr. Ser, vol. 143, edited by A. Bonaccorso et al., pp. 29-47, AGU, Washington, D.C.

Branca, S., Abate, T., 2017. Current knowledge of Etna's flank eruptions (Italy) occurring over the past 2500years. From the iconographies of the XVII century to modern geological cartography. Journal of Volcanology and Geothermal Research 1-19Bragagnia,A., Avanzinelli, R., Freymuth, H., Francalanci, L., 2014. Recycling of crystal mush-derived melts and short magma residence times revealed by U-series disequilibria at Stromboli volcano. Earth and Planetary Science Letters, 404, 206–219

Branca, S., Del Carlo, P., 2004. Eruptions of Mt. Etna during the past 3200 years: A revised compilation integrating the historical and stratigraphic records, in Mt. Etna: Volcano Laboratory, Geophys. Monogr. Ser, vol. 143, edited by A. Bonaccorso et al., pp. 1 – 27, AGU, Washington, D. C

Burton, M.R., Neri, M., Andronico, D., Branca, S., Caltabiano, T., Calvari, S., Corsaro, R.A., Del Carlo, P., Lanzafame, G., Lodato, L., Miraglia, L., Salerno, G., Spampinato, L., 2005. Etna 2004–2005: an archetype for geodynamically-controlled effusive eruptions. Geophysical Research Letters 32, 9

Calvari, S., Behncke, B., 2006. Etna: next term lava flows from multiple vents during 22 September to 4 November. Bull Glob Volcanism Netw 31 (10), 2-3

Calvari, S., Behncke, B., 2007. Etna: next term episodes of eruptions continue between 4 November and 14 December 2006. Bull Glob Volcanism Netw 32 (2), 22-26

Calvari, S., Coltelli, M., Neri, M., Pompilio, M., Scribano, V., 1994.The 1991–1993 Etna eruption: chronology and lava flow-field evolution. Acta Volcanology 4, 1-14

Calvari, S., Lodato, L., Neri, M., Behncke, B., Norini, G., Consoli, O., 2006. Changes in morphology of SE Crater and the emission of lava flows to the SSE. Bull Glob Volcanism Netw 31(8), 2-3

Calvari, S., Neri, M., Pinkerton, H., 2003. Effusion rate estimations during the 1999 summit eruption on Mt. Etna, and growth of two distinct lava flow fields. J. Volcanol. Geoth. Res. 119, 107-123

Carignan, J., Hild, P. , Mevelle, G., Morel, J., Yeghicheyan, D., 2001. Routine analyses of trace elements in geological samples using flow injection and low pressure on-line liquid

chromatography coupled to ICP-MS: A study of geochemical reference materials BR, DR-N, UB-N, AN-G and GH, Geostand. Newsl. 25, 187 -198

Chester, D.K., Duncan, A.M., Guest, J.E., Kilburn, C.R.J., 1985. Mount Etna, the Anatomy of a Volcano, Chapman and Hall, London.

Clocchiatti, R., Condomines, M., Guènot, N., Tanguy, J.C., 2004. Magma changes at Mount Etna: the 2001 and 2002–2003 eruptions. Earth and Planetary Science Letters 226, 397-414

Collins, S.J., Pyle, D.M., Maclennan J., 2009. Melt inclusions track pre-eruption storage and dehydration of magmas at Etna. Geology 37, 571-574

Coltelli, M., Del Carlo, P., Vezzoli, L., 2000. Stratigraphic constrains for explosive activity in the last 100 ka at Etna volcano, Italy. International Journal of Earth Sciences 89, 665-677

Coltelli, M., Del Carlo, P., Pompilio, M., Vezzoli, L., 1998. Discovery of a Plinian basaltic eruption of Roman age at Etna volcano, Italy. Geology 26, 1095-1098

Coltelli, M., Del Carlo, P., Pompilio, M., Vezzoli, L., 2005. Explosive eruption of a picrite: The 3930 BP subplinian eruption of Etna volcano (Italy). Geophysical Research Letters 32, L23307

Correale, A., Paonita, A., Martelli, M., Rizzo, A., Rotolo, S., Corsaro, R.A., Di Renzo, V., 2014. A two-component mantle source feeding Mt. Etna magmatism: insights from the geochemistry of primitive magmas. Lithos 184-187, 243-258

Corsaro, R.A., Andronico, D., Behncke, B., Branca, S., Caltabiano, T., Ciancitto, F., Cristaldi, A., De Beni, E., La Spina, A., Lodato, L., Miraglia, L., Neri, M., Salerno, G.,Scollo, S., Spata,G., 2017. Monitoring the December 2015 summit eruptions of Mt. Etna (Italy): Implications on eruptive dynamics. J. Volcanol. Geoth. Res. 341, 53-69.

Corsaro, R.A., Civetta, L., Di Renzo, V., Miraglia, L., 2009 a. Petrology of lavas from the 2004–2005 flank eruption of Mt. Etna, Italy: inferences on the dynamics of magma in the shallow plumbing system. Bull. Volcanol. 71,781-793

Corsaro, R.A., Cristofolini, R., 1993. Nuovi dati petrochimici ed isotopici sulla successione del Mongibello recente (M.te Etna). Boll Acc Gioenia Sci Nat 26, 341, 185-225

Corsaro, R.A., Cristofolini, R., Patanè, L., 1996. The 1669 eruption at Mount Etna: chronology, petrology and geochemistry, with inferences on the magma sources and ascent mechanism.Bull. Volcanol. 58, 348-358

Corsaro, R.A., Di Renzo, V., Distefano, S., Miraglia, L., Civetta, L., 2013. Relationship between magmatic processes in the plumbing system of Mt. Etna and the dynamics of the eastern flank:

inferences from the petrologic study of the products erupted from 1995 to 2005. J. Volcanol. Geoth. Res. 251, 75-89

Corsaro, R.A., Métrich, N., 2016. Chemical heterogeneity of Mt. Etna magmas in the last 15ka. Inferences on their mantle sources. Lithos 252-253, 123-134

Corsaro, R.A., Métrich, N., Allard, P., Andronico, D., Miraglia, L., Fourmentraux, C., 2009 b. The 1974 flank eruption of Mount Etna: An archetype for deep dike-fed eruptions at basaltic volcanoes and a milestone in Etna's recent history. Journal of Geophysical Research 114, B07204

Corsaro, R.A., Miraglia, L., 2014. The transition from summit to flank activity at Mt. Etna, Sicily (Italy): Inferences from the petrology of products erupted in 2007–2009. J. Volcanol. Geoth. Res. 275, 51-60

Corsaro, R.A., Miraglia, L., Pompilio, M., 2007. Petrologic evidence of a complex plumbing system feeding the July–August 2001 eruption of Mt. Etna, Sicily, Italy. Bulletin of Volcanology 69 (4): 401-421

Corsaro, R.A., Pompilio, M., 2004. Magma dynamics in the shallow plumbing system of Mt. Etna as recorded by compositional variations in the volcanics of recent summit activity (1995–1999). J Volc Geotherm Res 137, 55-71

Corsaro, R.A., Rotolo, S.G., Cocina, O., Tumbarello, G., 2014. Cognate xenoliths in Mt. Etna lavas: witnesses of the high velocity body beneath the volcano. Bull. Volcanol. 76, 772

Coulson, I.M., Stuart, F.M., MacLean, N.J., 2011. Assessing the link between mantle source and sub-volcanic plumbing in the petrology of basalts from 2001 and 2002/2003 eruptions of Mount Etna, Sicily: evidence from geochemical and helium isotope data. Lithos 123, 254-261

Di Muro, A., Métrich, N., Vergani, D., Rosi, M., Armienti, P., Fougeroux, T., Deloule, E., Arienzo, I., Civetta, L. 2014. The Shallow Plumbing System of Piton de la FournaiseVolcano (La Reunion Island, Indian Ocean) Revealed by the Major 2007 Caldera-Forming Eruption. Journal of Petrology 55, 1287-1315

Faure, G. (1986) Principles of isotope geology. Second edition. Editor Wiley & Sons, pp.589

Ferlito, C., 2017. Mount Etna volcano (Italy). Just a giant hot spring! Earth Science Reviews 177,14-23

Ferlito, C., Coltorti, M., Cristofolini, R., Giacomoni, P.P., 2009a. The contemporaneous emission of low-K and high-K trachybasalts and the role of the NE Rift during the 2002 eruptive event, Mt. Etna, Italy. Bull. Volcanol. 71, 575-587

Ferlito, C., Coltorti, M., Lanzafame, G., Giacomoni, P.P., 2014. The volatile flushing triggers eruptions at open conduit volcanoes: Evidence from Mount Etna volcano (Italy). Lithos 184, 447-455

Ferlito, C., Lanzafame, G., 2010. The role of supercritical fluids in the potassium enrichment of magmas at Mount Etna volcano (Italy). Lithos 119, 642-650

Ferlito, C., Viccaro, M., Cristofolini, R., 2009b. Volatile-rich magma injection into the feeding system during the 2001 eruption of Mt. Etna (Italy): its role on explosive activity and change in rheology of lavas. Bull. Volcanol. 71, 1149-1158

Ferlito, C., Viccaro, M., Nicotra, E., Cristofolini, R., 2012. Regimes of magma recharge and their control on the eruptive behaviour during the period 2001–2005 at Mt. Etna volcano. Bull. Volcanol. 74, 533-543

Fornaciai, A., Perinelli, C., Armienti, P., Favalli, M., 2015. Crystal size distributions of plagioclase in lavas from the July–August 2001 Mount Etna eruption. Bull. Volcanol. 77, 70-15Francalanci, L., Avanzinelli, R., Nardini, I., Tiepolo, M., Davidson, J.P., Vannucci, R., (2012). Crystal recycling in the steady-state system of the active Stromboli volcano: a 2.5-ka story inferred from in situ Sr-isotope and trace element data. Contrib Mineral Petrol., 163, 109–131

Giacomoni, P.P., Coltorti, M., Bryce, J.G., Fahnestock, M. F., Guitreau, M., 2016. Mt. Etna plumbing system revealed by combined textural, compositional, and thermobarometric studies in clinopyroxenes. Contrib. Mineral. Petr. 171,1-15

Giacomoni, P.P., Ferlito, C., Alesci, G., Coltorti, M., Monaco, C., Viccaro, M., Cristofolini, R., 2012. A common feeding system of the NE and S rifts as revealed by the bilateral 2002/2003 eruptive event at Mt. Etna (Sicily, Italy). Bull. Volcanol. 74, 2415-2433

Giacomoni, P.P., Ferlito, C., Coltorti, M., Bonadiman, C., lanzafame, G., 2014. Plagioclase as archive of magma ascent dynamics on “open conduit” volcanoes: The 2001-2006 eruptive period at Mt. Etna. Earth Science Reviews 138, 371-393

Giuffrida, M., Holtz, F., Vetere, F., Viccaro, M., 2017. Effects of CO_2 flushing on crystal textures and compositions: experimental evidence from recent K-trachybasalts erupted at Mt. Etna.,4 Contrib Mineral Petrol 172, 90

Giuffrida, M., Viccaro, M., 2017. Three years (2011–2013) of eruptive activity at Mt. Etna_ Working modes and timescales of the modern volcano plumbing system from micro-analytical studies of crystals. Earth Science Reviews 171, 289-322

Giuffrida, M., Viccaro, M., Ottolini, L., 2018. Ultrafast syn-eruptive degassing and ascent trigger high-energy basic eruptions. Scientific Reports 8, 147

Goldstein, S.L., Deines, P., Oelkers, E.H., Rudnick, R.L., Walter, L.M., 2003. Standards for publication of isotope ratio and chemical data in Chemical Geology. Chemical Geology 202, 1-4

Joron, J. L., Treuil, M., 1984. Etude géochimique et pétrogenèse des laves de l'Etna, Sicile, Italie. Bull. Volcanol. 47, 1125-1144

Kahl, M., Chakraborty, S., Costa, F., Pompilio, M., 2011. Dynamic plumbing system beneath volcanoes revealed by kinetic modeling, and the connection to monitoring data: An example from Mt. Etna. Earth Planet Sc Lett 308,11-22

Kahl, M., Chakraborty, S., Costa, F., Pompilio, M., Liuzzo, M., Viccaro, M., 2013. Compositionally zoned crystals and real-time degassing data reveal changes in magma transfer dynamics during the 2006 summit eruptive episodes of Mt. Etna. Bulletin of Volcanology 75, 2,1-14

Kahl, M., Chakraborty, S., Pompilio, M., Costa, F., 2015. Constraints on the Nature and Evolution of the Magma Plumbing System of Mt. Etna Volcano (1991–2008) from a Combined Thermodynamic and Kinetic Modelling of the Compositional Record of Minerals. Journal of Petrology 56, 10, 2025-2068

Kahl, M., Chakraborty, S., Pompilio, M., Costa, F., 2016. Corrigendum to: "Constraints on the Nature and Evolution of the Magma Plumbing System of Mt. Etna Volcano (1991–2008) from a Combined Thermodynamic and Kinetic Modelling of the Compositional Record of Minerals." Jour of Petrol 57, 621-622

Landi, P., Corsaro, R.A., Francalanci, L., Civetta, L., Miraglia, L., Pompilio, M., Tesoro, R., (2009). Magma dynamics during the 2007 Stromboli eruption (Aeolian Islands, Italy): Mineralogical, geochemical and isotopic data. Journal of Volcanology and Geothermal Research 182, 255–268

Langmuir, C.H., Vocke, Jr. R.D., Hanson, G.N., Hart, S.R., 1978. A general mixing equation with applications to icelandic basalts. Earth and Planetary Science Letters 37, 380-392

Landi, P., Corsaro, R.A., Francalanci, L., Civetta, L., Miraglia, L., Pompilio, M., Tesoro, R., 2009. Magma dynamics during the 2007 Stromboli eruption (Aeolian Islands, Italy): Mineralogical, geochemical and isotopic data. Journal of Volcanology and Geothermal Research 182, 255-268

Le Maitre, R.W. 2002. Igneous rocks. A classification and glossary of terms, Recommendations of the IUGS Subcommission on the Systematics of Igneous Rocks, 2nd edn. Cambridge University Press, p. 236.

Métrich N, Rutherford M J(1998) Low pressure crystallization paths of H2O-saturated basaltic-hawaiitic melts from Mt. Etna: Implications for open-system degassing volcanoes. Geochim. Cosmochim. Acta 62, 1195–1205 non citato

Métrich, N., Allard, P., Spilliaert, N., Andronico, D., Burton, M., 2004. 2001 flank eruption of the alkali- and volatile-rich primitive basalt responsible for Mount Etna's evolution in the last three decades. Earth and Planetary Science Letters 228, 1-17

Middlemost, E.A.K., 1989. Iron oxidation ratios, norms and the classification of volcanic rocks. Chemical Geology, 77, 19-26

Mollo S., Blundy J., Scarlato P., De Cristofaro S.P., Tecchiato V., Di Stefano F., Vetere F., Holtz F., Bachmann O., 2018, An integrated P-T-H2O-lattice strain model to quantify the role of clinopyroxene fractionation on REE+Y and HFSE patterns of mafic alkaline magmas: Application to eruptions at Mt. Etna. Earth-Science Reviews, 185, 32-56,

Mollo, S., Giacomoni, P.P., Coltorti, M., Ferlito, C., Iezzi, G., Scarlato, P., 2015. Reconstruction of magmatic variables governing recent Etnean eruptions: Constraints from mineral chemistry and P-T-fO(2)-H2O modeling. Lithos 212, 311-320

Moretti, R., , Métrich, N., Arienzo, I., Di Renzo, V., Aiuppa, A., Allard, P., 2018. Degassing vs. eruptive styles at Mt. Etna volcano (Sicily, Italy). Part I: Volatile stocking, gas fluxing, and the shift from low-energy to highly explosive basaltic eruptions. Chemical Geology https://doi.org/10.1016/j.chemgeo.2017.09.017.

Morgavi, D., Perugini, D., De Campos, C. P., Ertel-Ingrisch, W., Dingwell, D. B., 2013. Time evolution of chemical exchanges during mixing of rhyolitic and basaltic melts. Contrib. to Mineral. Petrol. 166, 615-638

Neri, M., Acocella, V., 2006. The 2004-05 Etna eruption: implications for flank deformation and structural behaviour of the volcano. J Volcanol Geotherm Res158, 195-206

Nicotra, E., Viccaro, M., 2012. Transient uprise of gas and gas-rich magma batches fed the pulsating behavior of the 2006 eruptive episodes at Mt. Etna volcano. J. Volcanol. Geotherm. Res. 227–228, 102-118

Palano, M., Viccaro, M., Zuccarello, F., Gresta, S., 2017. Magma transport and storage at Mt. Etna (Italy): A review of geodetic and petrological data for the 2002-03, 2004 and 2006 eruptions.

Journal of Volcanology and Geothermal Research 347, 1-16

Patanè, D., Barberi, G., Cocina, O., De Gori, P., Chiarabba, C., 2006. Time resolved seismic tomography detects magma intrusions at Mount Etna. Science 313, 821-823

Patanè, D.,Aiuppa, A., Aloisi, M., Behncke, B., Cannata, A., Coltelli, M., Di Grazia, G., Gambino, S., Gurrieri, S., M. Mattia, M., Salerno, G., 2013.Insights into magma and fluid transfer at Mount Etna by a multiparametricapproach: Amodel of the events leading to the 2011 eruptive cycle. J. Geophys. Res. Solid Earth 118, 3519-3539

Peccerillo, A., 2017. Cenozoic Volcanism in the Tyrrhenian Sea Region. Second edition. Advances in Volcanology. Editor Karoly Nemeth, Springer International Publishing, pp. 399. DOI 10.1007/978-3-319-42491-0

Perinelli, C., Mollo, S., Gaeta ,M., De Cristofaro S. P., Palladino, D. M., Armiento, P., Scarlato, P., Putirka, K. D., 2016. An improved clinopyroxene-based hygrometer for Etnean magmas and implications for eruption triggering mechanisms. American Mineralogist 101, 2774-2777

Pietruszka, A.J., Garcia, M.O., 1999. The size and shape of KilaueaVolcano's summit magma storage reservoir: a geochemical probe.Earth Planet Sci Lett 167(3–4), 311-320

Pompilio, M., Bertagnini, A., Métrich, N., 2012. Geochemical heterogeneities and dynamics of magmas within the plumbing system of a persistently active volcano: evidence from Stromboli. Bulletin of Volcanology, 74, 881-894

Rittmann, A., 1965. Notizie sull'Etna. Supplemento al Nuovo Cimento 3(I):1117–1123

Ryan, M.P., 1988. The mechanics and three-dimensional internal structure of active magmatic systems: Kilauea Volcano, Hawaii, J. Geophys. Res., 93, 4213-4248

Schiavi, F., Rosciglione, A., Kitagawa, H., Kobayashi, K., Eizo Nakamura, E., Nuccio, P.M., Ottolini, L., Paonita, A.,Vannucci R., 2015. Geochemical heterogeneities in magma beneath Mount Etna recorded by 2001-2006 melt inclusions. Geochem Geophys Geosyst 16: 2109-2126

Spilliaert, N., Allard, P., Metrich, N., Sobolev, A.V., 2006. Melt inclusion record of the conditions of ascent, degassing, and extrusion of volatile-rich alkali basalt during the powerful 2002 flank eruption of Mount Etna (Italy). Journal of Geophysical Research: Solid Earth 111, B04203

Tanguy, J. C., 1980. L'Etna: Etude pétrologique et paléomagnetique implications volcanologiques, These de Doctorat d'état thesis, Université Pierre et Marie Curie (PARIS 6).

Thornber, C., 2003. Magma-reservoir processes revealed by geochemistry of the Pu'u 'O'o Kupaianaha eruption. USGS Prof Paper 1676, 121-136

Tonarini S., Armienti, P., D'Orazio, M., Innocenti, F., 2001. Subduction-like fluids in the genesis of Mt. Etna magmas: evidences from boron isotopes and fluid mobile elements. Earth and Planetary Science Letters 192 (4), 471-483

Tonarini, S., Armienti, P. , D'Orazio, M., Innocenti, F. , Pompilio, M., Petrini, R., 1995. Geochemical and isotopic monitoring of Mt.Etna 1989-93. Eruptive activity: bearing on the shallow feeding system, Journal of Volcanology and Geothermal Research64, 95-115

Ubide, T. and Kamper, B.S., 2018..Volcanic crystals as time capsules of eruption history. Nature Communications 9, 326

Viccaro M, Calcagno R, Garozzo I, Giuffrida, M., Nicotra, E., 2015.Continuous magma recharge at Mt. Etna during the 2011–2013 period controls the style of volcanic activity and compositions of erupted lavas. Mineralogy and Petrology. 109, 67-83

Viccaro, M., Cristofolini, R., 2008. Nature of mantle heterogeneity and its role in the short-term evolution of Mt. Etna (Italy). Lithos 105, 272-288

Viccaro M, Ferlito C, Cortesogno L, Cristofolini R, Gaggero L., 2006. Magma mixing during the 2001 event at Mount Etna (Italy): Effects on the eruptive dynamics. Journal of Volcanology and Geothermal Research 149, 139-159

Viccaro, M., Giacomoni, PP., Ferlito, C., Cristofolini, R., 2019. Dynamics of magma supply at Mt. Etna volcano (Southern Italy) as revealed by textural and compositional features of plagioclase phenocrysts. Lithos 116, 77-91

Viccaro, M., Nicotra, E., Millar, I., Cristofolini, R., 2011. The magma source at Mount Etna volcano: perspective from the Hf isotope composition of historic and recent lavas. Chemical Geology 281, 343-351

Viccaro, M., Zuccarello, F., Cannata, A., Palano, D., Gresta, S., 2016. How a complex basaltic volcanic system works: Constraints from integrating seismic, geodetic, and petrological data at Mount Etna volcano during the July-August 2014 eruption. Journal of Geophysical Research Solid Earth 121, 5659-5678

Wadge, G., 1980. Flank fissures of Etna and the surface expressions of magmatic conduits, in United Kingdom Research on Mount Etna 1977–79, pp. 27– 30, R. Soc., London.

Figure captions

Figure 1

DEM of the Mt. Etna summit area with the location of the main craters (NEC= North-East Crater, SEC-NSEC=complex formed by South-East Crater and New South-East crater, VOR=Voragine, BN=Bocca Nuova), and the eruptive fissures of flank eruptions occurring in 2001 (UV= Upper Vents; LV= Lower Vents), 2002-03 (NF= Northern Fissures; SF= Southern Fissures), 2004-05 and 2008-09. VdB stands for Valle del Bove. The inset shows the regional setting of Mt. Etna.

Figure 2

Total alkali-silica classification diagram (Le Maitre, 2002) of products erupted during the 2001-2012 activity, with the inset focusing on the composition difference between sample 2002-A (hawaiite) and other 2001-2012 studied products (K-trachybasalts)**.**

Figure 3

SiO_2, CaO, alkali contents vs. Mg #(panels a, b, c) and Rb, La and Ni vs. Th content (panels d, e, f) of the products erupted during the 2001-2012 activity. The dotted line corresponds to the compositional field of the Etnean products erupted from 1995 to the onset of the 2001 flank eruption (data from Corsaro et al. 2013). In panel d, the dashed area corresponds to products erupted from 1928 to 1669 (from Joron and Treuil, 1984 in Corsaro et al. 2009). Error bars on element measurements are also reported**.**

Figure 4

Temporal variation of a) CaO/Al_2O_3 and b) La of products erupted during the 2001-2012 activity. Error bars on element measurements are also reported**.**

Figure 5

Temporal variation of a) $^{87}Sr/^{86}Sr$ and b) $^{143}Nd/^{144}Nd$of the products erupted during the 2001-2012 activity. Panel c) shows $^{87}Sr/^{86}Sr$ vs. $^{143}Nd/^{144}Nd$ of samples represented in a) and b). The red line encompasses the compositional field of lavas erupted after 1974 (Armienti et al. 2002, Clocchiatti et al. 2004; Viccaro and Cristofolini 2008; Corsaro et al. 2009a; Viccaro et al. 2011; Corsaro et al. 2013). Error bars on Sr and Nd isotopic ratio measurements are also reported**.**

Figure 6

Frequency histograms of $^{87}Sr/^{86}Sr$ of products erupted during the 2001-2012 activity integrated with literature analyses of samples erupted after 1974 (Armienti et al. 2004, 2007; Clocchiatti et al. 2004; Viccaro and Cristofolini 2008; Corsaro et al. 2009a; Viccaro et al. 2011; Corsaro et al. 2013). Red curves represent Gaussian curves calculated by Isoplot 3.00 (see text); the identified modes (green solid lines) and their fraction are reported in the legend.

Figure 7

$^{87}Sr/^{86}Sr$ of the products erupted during the 2001-2012 activity vs. a) Rb/Nb and b) Rb/Th ratios. Error bars on Sr isotopic ratio measurements and on element measurements are also reported**.**

Figure 8

$^{87}Sr/^{86}Sr$ vs. Nb content of products erupted during the activity at NEC of June-July 2002 (present study) and the period 1995 to 1999 (data from Corsaro et al. 2013). The mixing line (in red) is modeled according to Faure (1986, p. 142, equation 9.9). The end members are: sample CNE060696 ($^{87}Sr/^{86}Sr$=0.703556±6, Nb= 49.1 ppm) and sample 180701A ($^{87}Sr/^{86}Sr$=0.703664±7, Nb= 37.2 ppm); ticks on the mixing line are the proportions of the end member 180701A in the mixed magma. Error bars on Sr isotopic ratio measurements and on Nb measurements are also reported.

Figure 9

a) Rb/Th, b) Rb/Nb, c) Rb/La vs. $^{87}Sr/^{86}Sr$ of CC-type and DDF-type Etnean magmas erupted since 1329 (Corsaro and Cristofolini 1993; Corsaro et al. 1996; Tonarini et al. 2001; Armienti et al. 2002; Viccaro and Cristofolini 2008, Corsaro et al. 2009a, 2013, Nicotra and Viccaro 2012, Correale et al. 2014). The products of the 2001-2012 activity analyzed in this study are included. The compositions of the mafic xenolith (sample 311002A1) hosted in 2002 products and of the hawaiite (2002-A) erupted from NF in 2002 are plotted for comparison. The compositional ranges of components DDF 18th (blue area) and DDF 21st (grey area) have been represented.

Figure 10

Temporal variation of a)$^{87}Sr/^{86}Sr$, b) Rb/Th, c) Rb/La of CC-type and DDF-type Etnean magmas erupted since 1329 (Corsaro and Cristofolini 1993; Corsaro et al. 1996; Tonarini et al. 2001; Armienti et al. 2002; Viccaro and Cristofolini 2008, Corsaro et al. 2009a, 2013, Nicotra and Viccaro 2012, Correale et al. 2014). The products of the 2001-2012 activity analyzed in this study are included. The compositions of the mafic xenolith (sample 311002A1) hosted in 2002 products and of the hawaiite (2002-A) erupted from NF in 2002 are plotted for comparison. The compositional ranges of components DDF 18th (blue area) and DDF 21st (grey area) have been represented. The dashed vertical blue lines mark the 1763 and 1974 DDF-type eruptions.

Table 1

Major oxide, trace element contents and Sr-Nd isotopes in bulk rocks and glass of selected samples of 2001-2012 eruptive activity**.**

Table 2

Analyses of Sr-Nd isotopes in bulk rocks, glass, minerals of selected samples erupted from 2001 to 2009. The bulk rocks composition (major and trace elements) of these samples has been already published (see Reference).

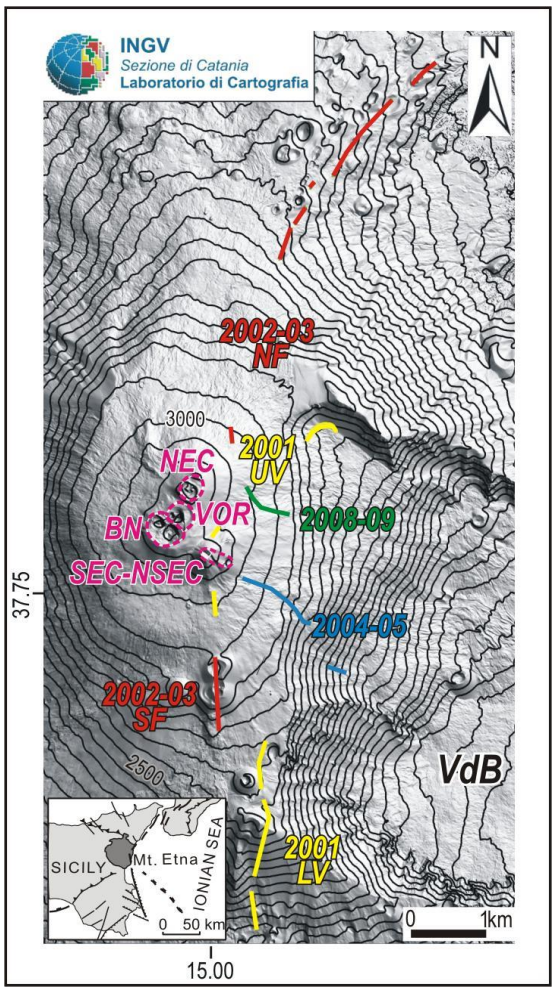

Figure 1

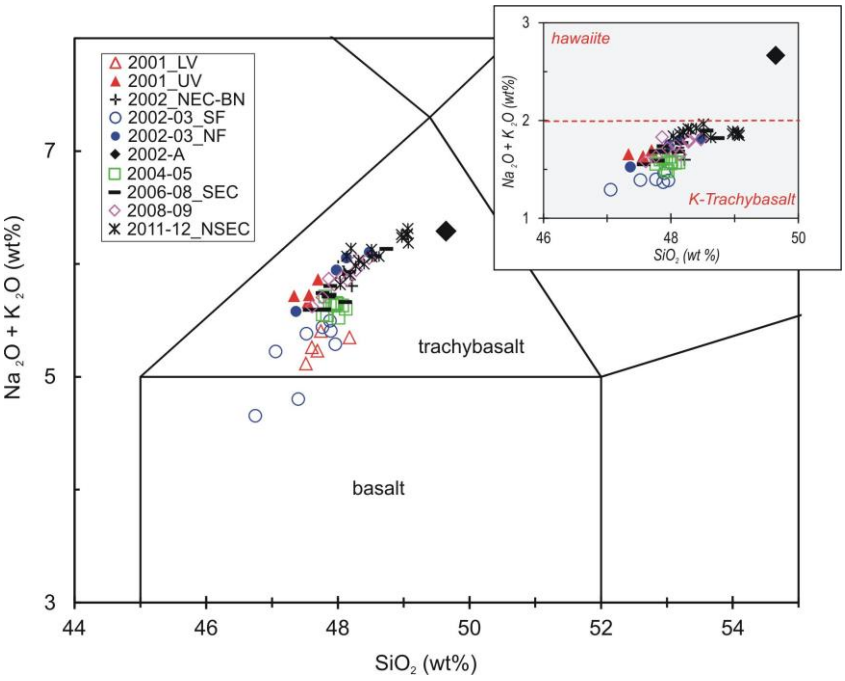

Figure 2

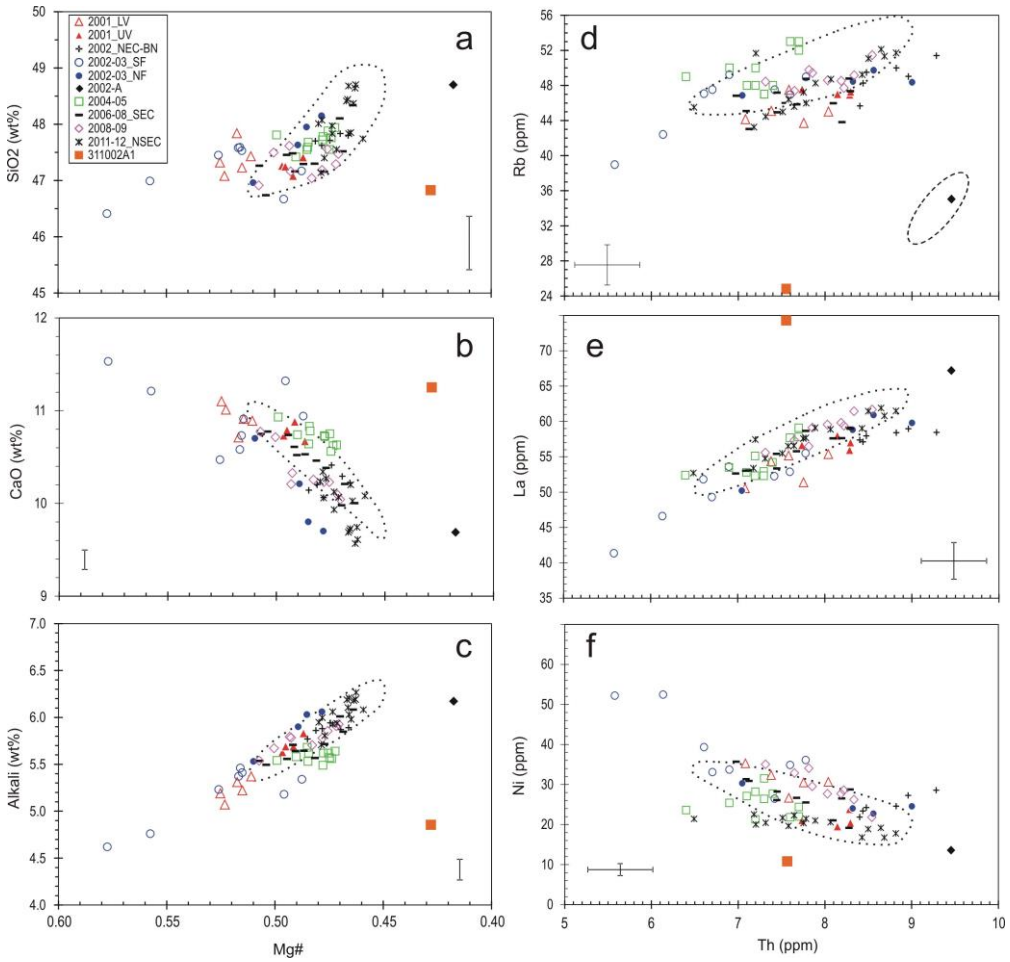

Figure 3

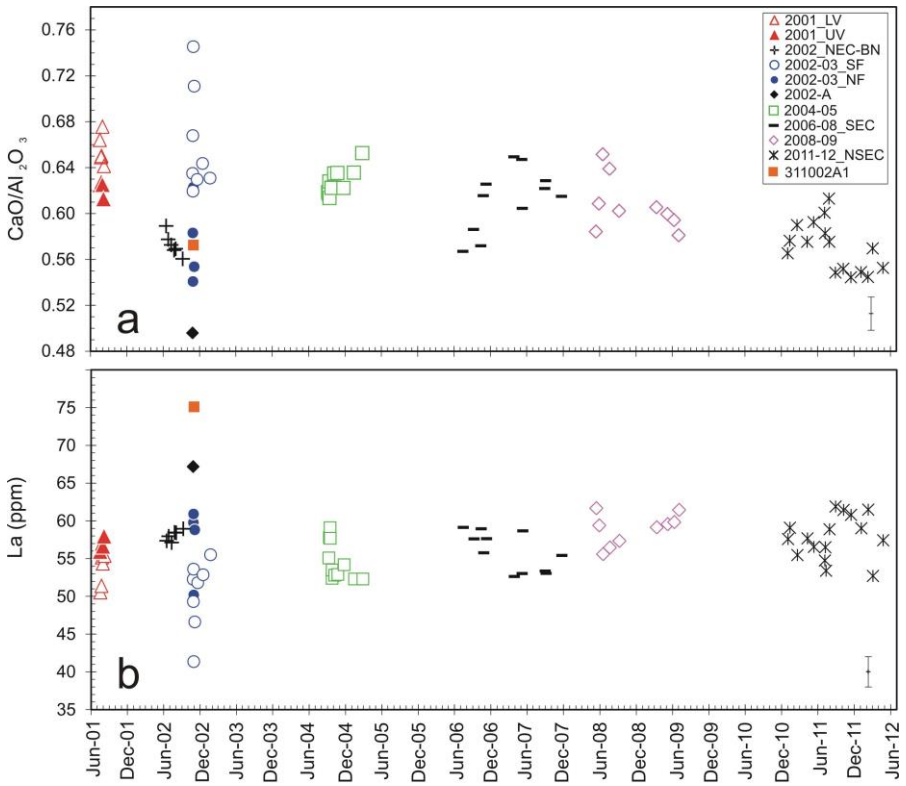

Figure 4

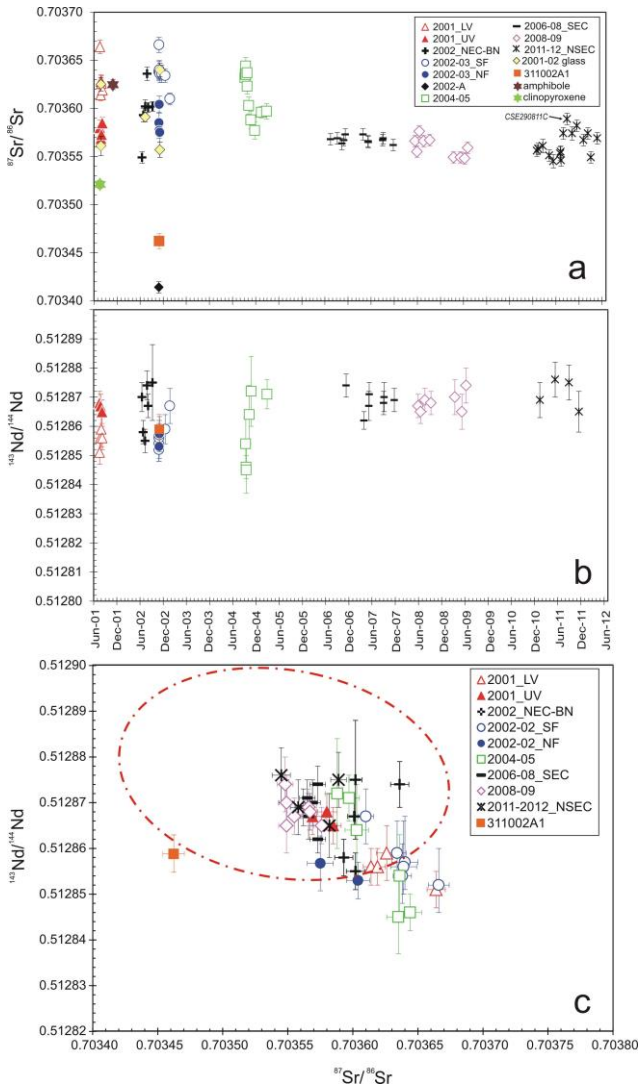

Figure 5

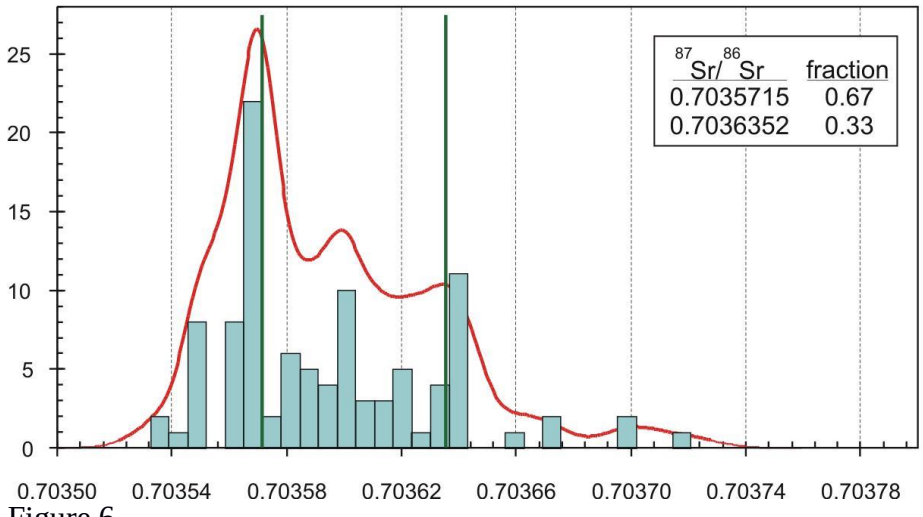

Figure 6

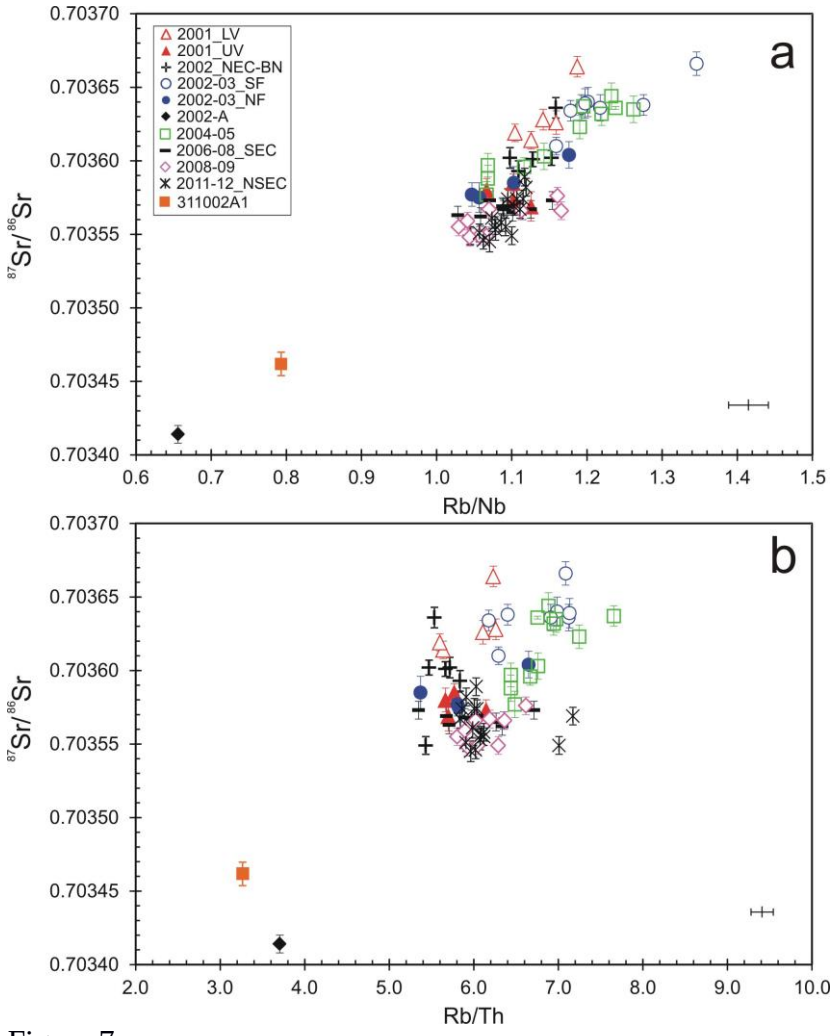

Figure 7

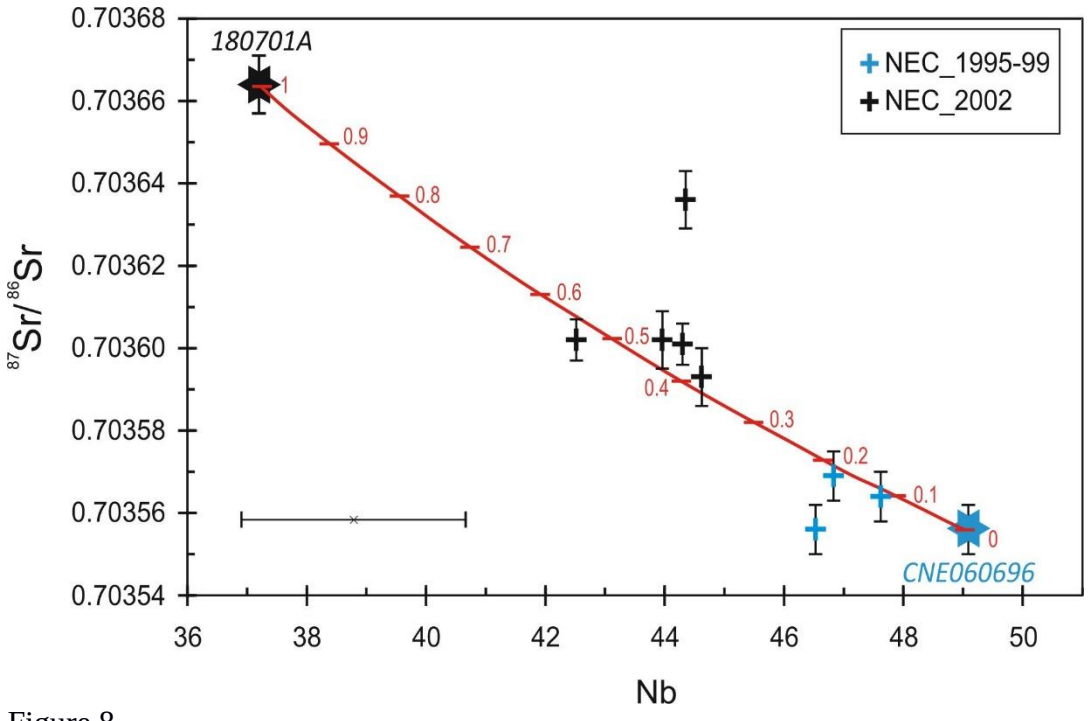

Figure 8

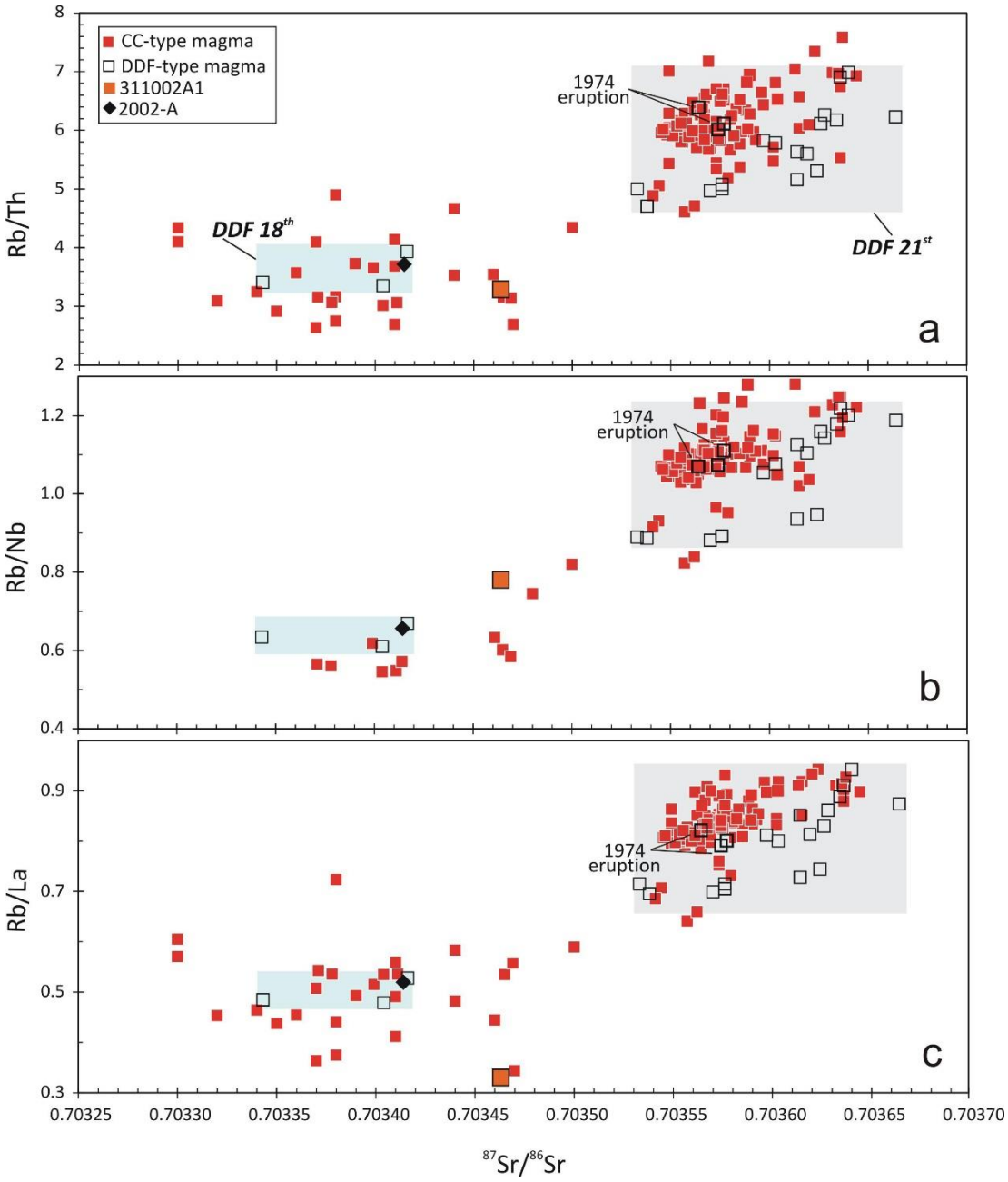
CC-type magma
DDF-type magma
311002A1
2002-A
1974 eruption
DDF 18th
DDF 21st
a
b
c
Rb/Th
Rb/Nb
Rb/La
87Sr/86Sr
0.70325
0.70330
0.70335
0.70340
0.70345
0.70350
0.70355
0.70360
0.70365
0.70370

Figure 9

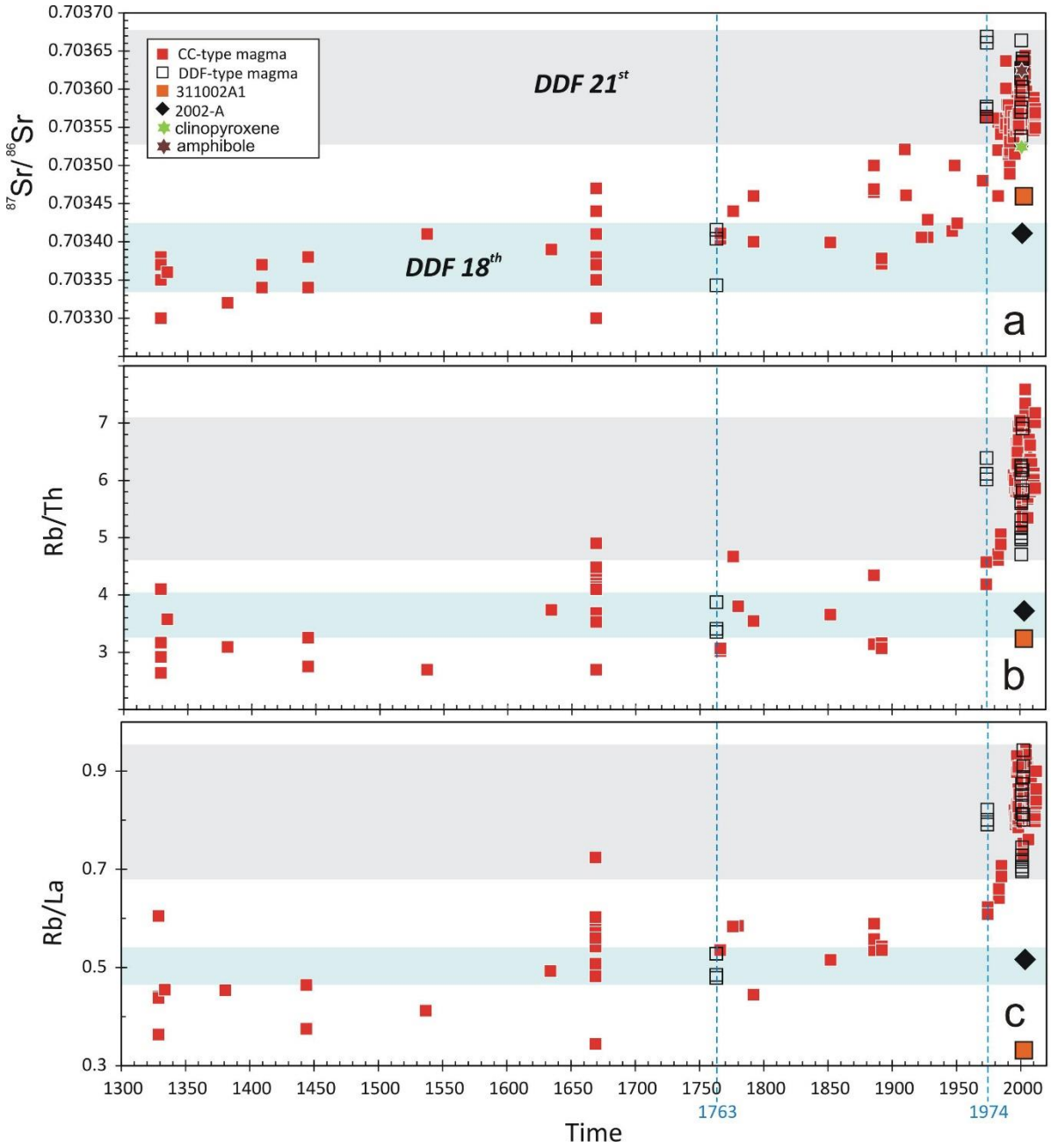
CC-type magma
DDF-type magma
311002A1
2002-A
clinopyroxene
amphibole
DDF 21st
DDF 18th
87Sr/86Sr
Rb/Th
Rb/La
a
b
c
Time
1763
1974

Figure 10

Table 1. (to be continued)

Sample	260701B	CNE260602	CNE110702	CNE070902C	301002R	161202	271002 LAP	2002-A	311002A1	150706B	CSE070906A	131006	261006B	091106C	CSE040907L	100609B
Eruption date	26-Jul-01	26-Jun-02	11-Jul-02	7-Sep-02	30-Oct-02	16-Dec-02	27-Oct-02	2002-03	2002-03	15-Jul-06	7-Sep-06	13-Oct-06	26-Oct-06	9-Nov-06	4-Sep-07	10-Jun-09
Type	lava flow	bomb	bomb	lapillo	bomb	lava flow	lapillo	bomb	mafic xenolith	lava flow	lava flow	lava flow	lava flow	lava flow	lava flow	lava flow
Crater/fissure [a]	2001_UV	NEC	NEC	NEC	2002-03_SF	2002-03_SF	2002-03_SF	2002-03		SEC	SEC	SEC	SEC	SEC	SEC	2008-09
Eruption type [b]	FL	SUM	SUM	SUM	FL	FL	FL	FL		SUM	SUM	SUM	SUM	SUM	SUM	FL
SiO_2	47.25	47.83	47.80	47.62	46.41	47.53	47.17	48.70	46.84	48.34	47.52	48.10	47.29	47.48	47.46	47.56
TiO_2	1.68	1.66	1.67	1.66	1.64	1.65	1.74	1.51	1.56	1.68	1.69	1.66	1.70	1.71	1.73	1.69
Al_2O_3	17.19	17.82	17.85	17.95	15.47	16.95	17.23	19.53	19.67	17.64	17.42	17.45	17.10	16.96	17.08	17.22
Fe_2O_3	1.74	1.71	1.71	1.71	1.81	1.72	1.77	1.40	1.64	1.65	1.70	1.68	1.73	1.76	1.74	1.69
FeO	8.69	8.53	8.57	8.53	9.04	8.59	8.85	7.01	8.18	8.26	8.51	8.42	8.64	8.78	8.69	8.44
MnO	0.17	0.17	0.17	0.17	0.17	0.17	0.17	0.16	0.16	0.18	0.18	0.18	0.18	0.18	0.18	0.18
MgO	5.64	5.00	4.95	5.17	8.17	6.04	5.57	3.33	4.06	4.73	4.96	4.94	5.42	5.62	5.62	5.06
CaO	10.79	10.29	10.22	10.06	11.53	10.91	10.94	9.69	11.25	10.00	10.21	9.98	10.53	10.61	10.74	10.23
Na_2O	3.66	3.79	3.80	3.79	2.93	3.40	3.36	4.39	3.71	3.94	3.80	3.94	3.66	3.69	3.62	3.81
K_2O	2.03	2.08	2.09	2.09	1.69	2.01	1.98	1.78	1.12	2.14	2.05	2.07	1.99	2.02	1.94	2.05
P_2O_5	0.50	0.53	0.55	0.52	0.42	0.54	0.48	0.60	1.13	0.62	0.61	0.63	0.59	0.59	0.57	0.60
L.O.I.	0.65	0.58	0.61	0.74	0.69	0.47	0.73	1.16	0.70	0.62	0.49	0.44	0.66	0.58	0.71	0.52
Total	99.99	99.99	100.00	100.00	99.96	99.97	99.98	99.26	100.02	99.80	99.14	99.49	99.48	99.97	100.06	99.03
Rb	47.3	49.5	48.3	49.0	39.0	46.9	47.5	35.0	24.7	48.8	46.0	47.3	45.8	43.8	43.0	48.5
Cs	0.86	0.93	0.94	0.97	0.69	0.91	0.92	0.67	0.49	0.89	0.85	0.84	0.81	0.87	0.79	0.85
Sr	1109	1171	1154	1149	950	1068	1095	1296	1623	1187	1139	1159	1144	1075	1087	1193
Ba	617	654	652	635	475	573	589	744	580	632	636	649	622	640	586	660
Ta	2.61	2.70	2.70	2.69	1.95	2.40	2.35	3.15	1.85	2.69	2.72	2.68	2.52	2.73	2.36	2.79
Th	8.30	8.48	8.44	8.96	5.58	7.60	7.42	9.46	7.55	8.28	8.10	8.29	7.68	8.20	7.13	8.19
U	2.47	2.50	2.46	2.60	1.62	2.20	2.18	2.68	1.99	2.38	2.38	2.40	2.23	2.40	2.09	2.38
Zr	197	213	212	210	171	197	195	217	117	214	199	211	201	194	191	219
Hf	4.59	4.63	4.64	4.57	4.03	4.40	4.38	4.52	2.86	4.58	4.53	4.46	4.43	4.84	4.20	4.70
Nb	42.0	44.6	44.0	42.5	32.4	39.8	37.3	53.4	32.0	44.8	42.3	46.0	42.1	40.9	39.4	46.5
La	57.0	57.9	57.1	59.0	41.4	52.9	52.3	67.2	75.1	59.1	57.6	59.0	55.8	57.6	53.1	59.8
Ce	110	115	114	113	88	102	102	125	148	110	110	112	108	110	101	115
Nd	47.9	49.3	49.3	48.4	40.9	45.3	45.6	50.3	66.3	49.0	47.7	48.0	47.0	48.8	43.8	49.5
Sm	9.44	9.26	9.26	9.20	8.18	8.80	8.95	8.94	12.13	9.20	9.23	8.97	9.06	9.29	8.55	9.31
Eu	2.91	2.81	2.74	2.81	2.50	2.70	2.73	2.73	3.37	2.77	2.74	2.72	2.68	2.79	2.65	2.83
Tb	1.04	1.05	1.04	1.04	0.90	0.99	1.03	0.96	1.19	1.00	1.02	0.98	1.02	1.06	0.97	1.04
Yb	2.17	2.25	2.24	2.23	1.94	2.20	2.18	2.15	2.17	2.17	2.18	2.14	2.13	2.25	2.05	2.28
Lu	0.34	0.33	0.33	0.34	0.28	0.32	0.32	0.32	0.32	0.33	0.33	0.33	0.33	0.33	0.31	0.33
Y	26.2	26.9	26.6	26.0	24.3	25.4	26.2	25.4	28.56	26.5	25.3	26.3	25.9	25.3	24.8	28.0
Ni	20.4	24.2	23.4	27.3	52.2	34.9	26.5	13.6	11.2	19.2	21.0	28.8	26.7	26.5	30.9	27.7
Cr	34.8	32.2	25.1	26.0	79.5	56.8	41.7	10.0	< L.D.	21.6	21.6	21.2	30.9	33.3	53.3	31.8
V	298	293	290	287	285	287	321	216	242	286	264	281	291	276	294	295
Co	36.8	37.0	36.4	36.2	43.6	38.0	39.4	25.6	28.1	33.8	32.7	35.6	35.1	36.2	37.0	36.4
Cu	138	125	124	124	135	123	132	130	82	128	124	109	125	118	131	138
$^{87}Sr/^{86}Sr$ [c]	0.703569±10	0.703593±7	0.703602±7	0.703602±5	0.70364±10	0.703634±7	0.703638±7	0.703414±6	0.703462±8	0.703568±6	0.703569±6	0.703563±6	0.703567±6	0.703573±6	0.703569±6	0.703548±6
$^{87}Sr/^{86}Sr$ (gl) [d]	0.703561±10		0.703591±5													
$^{143}Nd/^{144}Nd$ [e]	0.512867±4	0.512858±4	0.512855±4	0.512875±13	0.512857±5	0.512859±5	0.512854±6		0.512859±5					0.512874±4	0.51287±5	0.512874±6

[a] crater/eruption: NEC is “North-East Crater”, SEC is "South-East Crater", BN is “Bocca Nuova Crater”. NSEC is "New South-East Crater". LV and UV are for 2001 Lower and Upper Vents (Corsaro et al, 2007); SF and NF are for 2002-03 Southern and Northern Fissures (Andronico et al., 2005)

[b] type of activity: “flank” (FL) and summit (SUM)

[c] Sr-isotopic ratio calculated for the whole rock. The quoted error (2s mean N=175) of the isotopes refers to the last digit

[d] Sr-isotopic ratio calculated for separated glasses

[e] Nd-isotopic ratio calculated for the whole rock. The quoted error (2s mean N=175) of the isotopes refers to the last digit

(continued)

Sample	CSE 020111A	CSE 120111D	CSE180211A	CSE100411A	CSE120511C	CSE060711	CSE090711F	BN120711A	CSE 300711D	CSE 290811C	CSE 081011	CSE 151111A	CSE050112C	CSE090212	CSE040312A	CSE240412F
Eruption date	2-Jan-11	12-Jan-11	18-Feb-11	10-Apr-11	12-May-11	6-Jul-11	9-Jul-11	12-Jul-11	30-Jul-11	29-Aug-11	8-Oct-11	15-Nov-11	5-Jan-12	9-Feb-12	4-Mar-12	24-Apr-12
Type	bomb	lava flow	lapillo	bomb	lava flow	bomb	bomb	bomb	lava flow	lava flow	bomb	bomb	lapillo	bomb	lava flow	bomb
Crater/fissure [a]	NSEC	NSEC	NSEC	NSEC	NSEC	NSEC	NSEC	NSEC	NSEC	NSEC	NSEC	NSEC	NSEC	NSEC	NSEC	NSEC
Eruption type [b]	SUM	SUM	SUM	SUM	SUM	SUM	SUM	SUM	SUM	SUM	SUM	SUM	SUM	SUM	SUM	SUM
SiO_2	47.74	47.83	47.83	47.97	48.01	47.40	47.55	47.14	48.07	48.68	48.41	48.37	48.64	48.70	47.85	48.44
TiO_2	1.69	1.70	1.71	1.69	1.70	1.70	1.70	1.71	1.66	1.65	1.65	1.65	1.66	1.67	1.67	1.64
Al_2O_3	17.83	17.70	17.16	17.26	17.28	17.09	17.27	16.98	17.49	17.73	17.55	17.57	17.75	17.64	17.60	17.57
Fe_2O_3	1.68	1.70	1.71	1.69	1.71	1.70	1.69	1.72	1.64	1.63	1.64	1.63	1.64	1.65	1.66	1.63
FeO	8.42	8.51	8.53	8.46	8.57	8.50	8.45	8.58	8.20	8.13	8.19	8.17	8.22	8.23	8.29	8.13
MnO	0.18	0.18	0.18	0.19	0.19	0.18	0.18	0.18	0.19	0.18	0.19	0.18	0.18	0.19	0.18	0.18
MgO	4.73	4.91	5.07	5.03	5.23	5.13	4.99	5.21	4.97	4.69	4.74	4.67	4.69	4.69	4.77	4.70
CaO	10.08	10.20	10.12	9.93	10.24	10.27	10.07	10.34	10.06	9.73	9.69	9.57	9.74	9.61	10.03	9.71
Na_2O	3.97	3.94	3.91	4.00	3.93	3.83	3.91	3.76	3.90	4.02	4.02	4.01	4.03	4.06	3.91	3.96
K_2O	2.11	2.09	2.02	2.06	2.02	1.98	2.03	1.95	2.10	2.18	2.17	2.17	2.16	2.20	2.07	2.14
P_2O_5	0.61	0.60	0.59	0.60	0.59	0.58	0.59	0.56	0.59	0.61	0.61	0.60	0.60	0.61	0.60	0.61
L.O.I.	0.79	0.66	0.85	0.59	0.55	0.82	0.71	0.70	0.67	0.91	0.62	0.84	0.58	0.89	0.49	0.57
Total	99.83	100.02	99.67	99.47	100.01	99.17	99.13	98.83	99.53	100.14	99.48	99.44	99.90	100.14	99.11	99.28
Rb	47.2	48.3	45.0	46.0	45.6	44.5	46.4	43.2	48.7	52.1	51.1	51.3	49.2	51.7	45.5	51.7
Cs	0.87	0.84	0.81	0.82	0.81	0.80	0.84	0.76	0.92	0.98	0.98	1.03	0.95	1.00	0.85	1.05
Sr	1253	1278	1176	1182	1194	1183	1206	1150	1241	1283	1249	1251	1242	1253	1208	1278
Ba	645	657	611	634	622	602	626	595	646	681	674	666	648	678	608	656
Ta	2.51	2.60	2.46	2.58	2.50	2.36	2.47	2.42	2.60	2.75	2.76	2.68	2.60	2.75	2.44	2.77
Th	7.75	7.89	7.51	7.78	7.65	7.32	7.58	7.18	8.07	8.65	8.50	8.69	8.43	8.82	6.49	7.20
U	2.29	2.31	2.19	2.28	2.21	2.10	2.18	2.11	2.33	2.48	2.46	2.42	2.32	2.43	1.81	2.02
Zr	211	214	201	205	202	200	203	195	215	227	222	221	236	223	175	225
Hf	4.47	4.42	4.35	4.38	4.44	4.22	4.38	4.26	4.66	4.73	4.77	4.62	4.55	4.75	4.42	4.85
Nb	43.8	44.4	41.9	43.5	42.6	41.2	42.5	40.7	43.7	46.7	46.6	45.9	44.3	46.7	41.4	46.8
La	57.6	59.1	55.5	57.7	56.5	54.7	56.5	53.4	58.9	61.9	61.4	60.8	59.0	61.5	52.7	57.4
Ce	107	110	106	108	107	104	107	100	107	113	112	109	105	110	107	117
Nd	47.8	48.5	46.1	46.9	47.2	45.9	47.0	44.8	48.7	51.0	50.3	50.6	48.8	51.4	46.7	51.1
Sm	8.99	9.35	8.80	8.77	8.80	8.72	8.91	8.68	9.37	9.71	9.43	9.31	9.16	9.50	8.90	9.73
Eu	2.77	2.85	2.69	2.71	2.71	2.65	2.69	2.63	2.81	2.92	2.85	2.86	2.78	2.92	2.74	2.92
Tb	1.00	1.03	0.97	0.99	0.99	0.98	1.00	0.96	1.04	1.07	1.05	1.05	1.03	1.06	0.99	1.08
Yb	2.10	2.18	2.07	2.09	2.09	2.09	2.13	2.02	2.24	2.33	2.27	2.26	2.22	2.29	2.12	2.33
Lu	0.31	0.32	0.32	0.31	0.32	0.32	0.32	0.31	0.33	0.35	0.34	0.34	0.34	0.34	0.31	0.35
Y	26.9	27.7	25.7	25.8	26.0	25.9	26.2	25.3	27.6	28.7	28.1	27.9	27.3	28.2	25.6	28.3
Ni	20.4	21.0	21.7	21.5	22.3	20.4	19.7	22.5	20.6	19.2	18.9	16.8	16.8	17.8	21.4	20.0
Cr	13.9	16.0	20.3	21.0	22.7	19.1	17.7	21.4	22.5	18.3	17.9	15.1	14.1	17.7	22.3	19.4
V	289	297	273	262	274	274	271	282	279	275	275	264	261	277	294	305
Co	34.5	45.9	38.7	39.8	39.5	36.9	37.0	38.3	38.2	46.9	37.8	36.6	35.4	37.1	36.8	37.8
Cu	144	141	127	124	125	126	127	127	116	114	119	110	120	119	122	102
$^{87}Sr/^{86}Sr$ [c]	0.703556±6	0.703558±6	0.703561±7	0.703551±6	0.703545±7	0.703553±7	0.703555±6	0.703546±6	0.703574±6	0.703589±6	0.703574±7	0.703582±6	0.703567±6	0.703574±6	0.703549±6	0.703569±6
$^{87}Sr/^{86}Sr$ (gl)																
$^{143}Nd/^{144}Nd$ [d]		0.512869±6			0.512876±6					0.512875±6		0.512865±7				

Table 2.

Sample	Eruption date	Type	Crater/fissure a	Eruption type	$^{87}Sr/^{86}Sr$ bulk rock	$^{87}Sr/^{86}Sr$ glass	$^{87}Sr/^{86}Sr$ amphibole	$^{87}Sr/^{86}Sr$ clinopyroxene	$^{143}Nd/^{144}Nd$ bulk rock	Reference
180701A	18-Jul-01	lava flow	2001_LV	FL	0.703664±7		0.703625±5	0.703521±4	0.512851±4	Corsaro et al., 2007
240701C	24-Jul-01	lapillo	2001_LV	FL	0.703614±6				0.512856±4	Corsaro et al., 2007
260701C	26-Jul-01	lava flow	2001_LV	FL	0.703628±7	0.703625±7				Corsaro et al., 2007
080801A	8-Aug-01	lava flow	2001_LV	FL	0.703619±6				0.512856±4	Corsaro et al., 2007
100801D	31-Jul-01	lava flow	2001_LV	FL	0.703626±8				0.512859±6	Corsaro et al., 2007
170701A	17-Jul-01	lapillo	2001_UV	FL	0.70358±8				0.512868±4	Corsaro et al., 2007
310701A	1-Aug-01	lava flow	2001_UV	FL	0.703573±7					Corsaro et al., 2007
60801	6-Aug-01	lava flow	2001_UV	FL	0.703585±6				0.512865±4	Corsaro et al., 2007
BN 160602	16-Jun-02	bomb	BN	SUM	*0.703549±6				0.51287±5	Corsaro et al., 2009a (aux. mater.)
CNE260702	26-Jul-02	bomb	NEC	SUM	0.703636±7				0.512874±5	Corsaro et al., 2009a (aux. mater.)
41102A	4-Nov-02	bomb	2002-03_SF	FL	*0.703636±9	0.703640±7				Corsaro et al., 2009a (aux. mater.)
281002F	28-Oct-02	lava flow	2002-03_NF	FL	0.703585±11					Corsaro et al., 2009a (aux. mater.)
41102B	4-Nov-02	lava flow	2002-03_NF	FL	*0.703575±10	0.703557±8			*0.512820±6	Corsaro et al., 2009a (aux. mater.)
CSE290307B	29-Mar-07	lava flow	SEC	SUM	0.703573±6				0.512862±3	Corsaro and Miraglia, 2013
CSE070507	7-May-07	lava flow	SEC	SUM	0.703566±6				0.512867±5	Corsaro and Miraglia, 2013
CSE310807A	31-Aug-07	bomb	SEC	SUM	0.703567±6				0.512868±4	Corsaro and Miraglia, 2013
CSE231107A	23-Nov-07	lava flow	SEC	SUM	0.703562±6				0.512869±4	Corsaro and Miraglia, 2013
CSE100508B	10-May-07	lava flow	SEC	SUM	0.703565±6				0.512871±4	Corsaro and Miraglia, 2013
140508B	14-May-08	bomb	2008-09	FL	0.703566±6					Corsaro and Miraglia, 2013
290508	29-May-08	bomb	2008-09	FL	0.703555±6				0.512867±4	Corsaro and Miraglia, 2013
170608	17-Jun-08	lava flow	2008-09	FL	0.703576±6				0.512865±4	Corsaro and Miraglia, 2013
210708	21-Jul-08	lava flow	2008-09	FL	0.703566±6				0.512869±4	Corsaro and Miraglia, 2013
070908	7-Sep-08	lava flow	2008-09	FL	0.703567±6				0.512868±4	Corsaro and Miraglia, 2013
140309	14-Mar-09	bomb	2008-09	FL	0.703549±6				0.512870±6	Corsaro and Miraglia, 2013
80509	8-May-09	lava flow	2008-09	FL	0.703549±6				0.512865±6	Corsaro and Miraglia, 2013
40709	3-Jul-09	lava flow	2008-09	FL	0.703559±6					Corsaro and Miraglia, 2013

*value published